F-65

AUBURN UNIVERSITY

IN-21550

FINAL REPORT

SOLID-PROPELLANT ROCKET MOTOR INTERNAL BALLISTICS PERFORMANCE VARIATION ANALYSIS (PHASE FIVE)

by

Richard H. Sforzini
Professor

and

Jesse E. Murph
Graduate Research Assistant

Aerospace Engineering Department

Prepared under

Modification No. 21-S1 to the Cooperative Agreement
Dated February 11, 1969, between
George C. Marshall Space Flight Center
NATIONAL AERONAUTICS AND SPACE ADMINISTRATION

and

AUBURN UNIVERSITY

Engineering Experiment Station
Auburn University
Auburn, Alabama 36830

January 1980

ENGINEERING

FINAL REPORT

SOLID-PROPELLANT ROCKET MOTOR INTERNAL BALLISTICS PERFORMANCE VARIATION ANALYSIS (PHASE FIVE)

by

Richard H. Sforzini
Professor

and

Jesse E. Murph
Graduate Research Assistant

Aerospace Engineering Department

Prepared under

Modification No. 21-S1 to the Cooperative Agreement
Dated February 11, 1969, between
George C. Marshall Space Flight Center
NATIONAL AERONAUTICS AND SPACE ADMINISTRATION

and

AUBURN UNIVERSITY

Engineering Experiment Station
Auburn University
Auburn, Alabama 36830

January 1980

SOLID-PROPELLANT ROCKET MOTOR INTERNAL BALLISTICS PERFORMANCE VARIATION ANALYSIS (PHASE FIVE)

Richard H. Sforzini and Jesse E. Murph

ABSTRACT

The report presents the results of research aimed at improving the predictability of internal ballistics performance of solid-propellant rocket motors (SRM's) including thrust imbalance between two SRM's firing in parallel. Static test data from the first six Space Shuttle SRM's is analyzed using a computer program previously developed for this purpose. The program permits intentional minor design biases affecting the imbalance between any two SRM's to be removed. Results for the last four of the six SRM's, with only the propellant bulk temperature as a non-random variable, are generally within limits predicted by theory. Extended studies, of internal ballistic performance of single SRM's are presented based on an earlier developed mathematical model which includes an assessment of grain deformation. The erosive burning rate law used in the model is upgraded and made more general. Excellent results are obtained in predictions of the performances of five different SRM's of quite different sizes and configurations. These SRM's all employ PBAN type propellants with ammonium perchlorate oxidizer and 16 to 20% aluminum except one which uses carboxyl terminated butadiene binder. The only non-calculated parameters in the burning rate equations that are changed for the different SRM's are the zero crossflow velocity burning rate coefficients and exponents. The results, in general, confirm the importance of grain deformation. The improved internal ballistic model makes practical the development of an effective computer program for application of an optimization technique to SRM design which is also demonstrated. The program uses a pattern search technique to minimize the difference between a desired thrust-time trace and one calculated based on the internal ballistic model. Up to fourteen design parameters may be varied for a single design problem in the search for the "best match." The program is demonstrated by matching the thrust-time trace obtained from static tests of the first Space Shuttle SRM starting with input values of 10 variables which are, in general, 10% different from the as-built SRM. An excellent match is obtained; final values are for the most part within a few percent of the as-built values. Computer operating time for the demonstration is less than 34 min. on the IBM 3031. The pattern search technique is also applied in an investigation aimed at improving the predictability of ignition transients by minimization of the difference between the actual chamber pressure of a Space Shuttle SRM and that calculated by the computer program of Caveny. Here the search parameters are the (poorly known) heat transfer coefficients applicable to various portions of the propellant surface during ignition. The set of coefficients that give the best match between predicted and calculated results are significantly different from those of the original analysis and yield a much improved prediction. Extensions suggested by the present research in the various key areas are identified.

ACKNOWLEDGEMENTS

The authors express appreciation to personnel at the George C. Marshall Space Flight Center (MSFC) for their many useful suggestions which materially aided this investigation and in particular to Mr. B. W. Shackelford, Jr., NASA Project Coordinator, who additionally provided data for the analyses and helpful encouragement to this research.

The participation of the following from the Aerospace Engineering Department at Auburn University is likewise acknowledged with appreciation: Mr. G. H. Conover, graduate research assistant, who performed the Space Shuttle thrust imbalance numerical evaluations and constructed a laboratory device for cold-flow simulation of SRM internal flow fields; Mr. J. L. Berry, laboratory assistant, who completed a computer program for visual display of test data which he began while an employee of MSFC; and Mrs. M. N. McGee who typed the manuscript.

TABLE OF CONTENTS

LIST OF FIGURES

LIST OF FIGURES (CONT'D)

LIST OF TABLES

NOMENCLATURE

English Symbol	Definition	Units Used
a	Propellant burning rate coefficient	$in/sec\text{-}psi^n$
c	Constant in Dittus-Boelter relation (Eq. V-1)	——
c_4	Constant in modified burning rate law	$(sec^3/slug)^{1/2}$
c_p	Specific heat at constant pressure	$cal/gm\text{-}°K$
d_h	Hydraulic diameter	cm
D	Diameter	in
f	Weighting factor in objective function	——
F	Thrust	lbf
G	Mass flow rate per unit area	$slugs/sec\text{-}in^2$
h	Convective heating coefficient	$cal/sec\text{-}°K\text{-}cm^2$
L, L_{ref}	Flow length and reference flow length, respectively, in modified flame height burning rate law	in
M	Mach number	——
n	Burning rate exponent	——
P	Pressure	lbf/in^2
P_{cr}	Critical pressure in modified flame height	lbf/in^2
P_j	Penalty function of jth constraint	units vary
P_r	Prandtl number	——
R	Specific gas constant	$cal/gm\text{-}°K$
r	Burning rate	in/sec
r_o	Burning rate at zero velocity parallel to the surface	in/sec
t	Time	sec

NOMENCLATURE (Continued)

English Symbol	Definition	Units Used
T_{af}	Average gas film temperature	°K
u	Velocity parallel to the burning surface (Eq. V-1)	cm/sec
V_f	Flame-spreading speed	in/sec
W	Molecular weight	gm/g-mole
x_{seg}	Effective distance from leading edge	cm
z_o	Initial difference between web thickness at the head and nozzle ends of the controlling grain length	in
Greek Symbol		
δ	Indicates percent change in optimization variables	units vary
Δ	Change or difference in quality	——
Φ	Objective function	lbf^2
Subscripts		
i,j	Running indices for time points and constraints, respectively	
n	Nozzle end of grain at position of maximum flow Mach number	
p	Port	
Superscripts		
*	Value of a variable where M=1	
-	Average or mean value	

I. INTRODUCTION AND SUMMARY

This report presents the results of research performed at Auburn University during the period January 12, 1979, to January 10, 1980, under Modification No. 21-S1 to the Cooperative Agreement dated February 11, 1969, between NASA Marshall Space Flight Center (MSFC) and Auburn University. The goal of this research is to resolve discrepancies between predicted ballistic performance of solid rocket motors (SRM's) and actual test results to include the thrust imbalance of pairs of SRM's firing in parallel as on the booster stage of the Space Shuttle. Attainment of this goal will lead to improved methods of both design and performance predictions for SRM's, demonstration of which is within the scope of this research.

The theoretical thrust imbalance of SRM's has been previously investigated statistically by application of the Monte Carlo technique.[1-6] Theoretical assessments of imbalance characteristics for Titan IIIC SRM's using computer programs described in Refs. 1 through 5 compare favorably with actual performance data.[2-4] However, the only Space Shuttle experimental data that was analyzed as a part of this previous effort was that from the static firings of the first two SRM's. Additional verification of the theoretical method is provided in the present research through examination of the static test data for Space Shuttle development motors (DM's) 1 through 4 and qualification motors (QM's) 1 and 2.

Different pairs of SRM's are formed by selecting combinations of individual SRM's taken two at a time. The thrust imbalance characteristics of these pairs are analyzed using a computer program previously developed for this purpose.[2] The program permits certain intentional design biases affecting the imbalance between any two SRM's to be removed. Results are compared with an earlier theoretical assessment obtained from the Monte Carlo analysis. With several of the pairs of DM's, the Monte Carlo computed limits are exceeded, but these discrepancies are explicable in terms of design changes within the pairs not accounted for in the computer program. A final assessment is made with the six combinations of DM-3 and 4 and QM-1 and 2 which gives results generally consistent with the Monte Carlo prediction.

During the earlier investigation of thrust imbalance, much effort was directed toward improving the predictability of performance of single SRM's because it is apparent that the ability to predict thrust imbalance characteristics is contingent on having an accurate model of the individual motors. The studies showed that a major improvement to performance predictability may be possible by considering the effects of grain deformation on the internal ballistics and by using a new burning rate model developed during the studies.[2-3] Comparisons of results of this approach with test data on a number of SRM's including the Space Shuttle SRM's were quite favorable. However, the burning rate model lacked generality in

that the erosion constants had to be adjusted for various SRM's to yield reasonable predictions even when the identical propellant was used in the several configurations.

In the present research, a refined empirical burning rate model is developed which extends greatly the generality of the original modified flame height burning rate equations. Excellent results were obtained with this equation in predicting the performance of the 5 different SRM's: the TU-455.02, the Castor (the TX354-5), the Titan IIIC boosters, the Space Shuttle boosters, and the associated 5-in. dia. ballistic test motors for the Space Shuttle. These SRM's all use high solids level propellants with ammonium perchlorate oxidizer and polybutadiene-acrylic acid-acrylonitrile terpolymer binder (PBAN) except for the Castor which uses a carboxyl terminated butadiene binder. The propellants all contain from 16 to 20% aluminum. The general results of the internal ballistic analyses also tend to support the hypothesis that grain deformation can significantly affect the ballistic performance of SRM's.

A related feature of the internal ballistics that needs to be explained is the special effect of the mixing of the gases generated by the burning of the aft end of the propellant with those of the main stream. Previous theoretical analyses of this phenomenon proved inconclusive.[2] As a part of the present research, an experimental cold-flow model was designed and constructed from existing hardware to be used in assessing losses in total pressure associated with the mixing for relatively simple grain geometries. Additional efforts under this project were restricted to directing the research of a graduate student performing research for his master's thesis in this area. Results will be reported in the thesis.

Another aspect of single SRM performance that is treated in the new research effort is the application of optimization techniques to internal ballistic analyses to enable selection of motor designs with desired characteristics. In previously MSFC sponsored research[7] the pattern search technique[8] has been applied with some success to design of igniters and analysis of ignition transients.[2,7] Based on the work of Woltosz[9] it appears that the same technique has merit for the present problem of selection of an optimum set of design parameters that will meet motor performance requirements such as that required to upgrade the capability of the Space Shuttle. However, the demonstration of this capability by Woltosz involved solution of a problem of limited scope. In the present work, the computer program developed by Woltosz has been extensively modified and broadened. The major extensions are: 1) the inclusion of the grain deformation analysis and new burning rate model in the internal ballistics subroutine, 2) the restoration, to the internal ballistics subroutine, of the input option which permits representation of special propellant burning geometry through the use of tabular values of burning surface versus distance burned, 3) the improvement of the pattern search technique to provide much more rapid convergence to the minimum objective function, 4) the addition of a third option for an optimization criterion. The original program options were: 1) maximize the ratio of total impulse to motor weight, or 2) mini-

mize the motor weight. Both options were subject to the constraint of achieving a minimum burnt vehicle velocity based on a drag-free and gravity-free trajectory and no payload. The new option simply minimizes the sum of the squares of the differences between computed and desired thrust at specified (up to 20) time points. In other words, the third option is to select the design parameters that will give the best match between a desired thrust-time trace and the predicted performance without regard to overall vehicle performance.

How well actual performance for an SRM designed with the selected parameters matches the desired performance will clearly depend on the goodness of the mathematical model of the internal ballistics. On the other hand, because of the large number of complete ballistic analyses necessary in the search for the best match, of desired and calculated values, a concise analysis is desirable. The model used is the simplified design analysis program[10,11] previously developed for MSFC but modified to include grain deformation effects[2,3,4] and the empirical modified burning rate model of the present research. As demonstrated in this report, by use of Space Shuttle SRM actual test data as desired thrust-time in the optimization program, excellent results are obtained in that the optimization variables selected by the program are very close to those actually used in construction of the SRM.

For the demonstration, in the interest of economy, only ten design parameters were permitted to vary. Computation time for this optimization was 33.15 minutes on the IBM 3031.

Ignition transient predictability receives additional consideration during the extended research. The ignition investigation is aimed at further improving the predictability of ignition characteristics of single SRM's and involves basically an extension of the work of Caveny.[12] Specifically, a new approach to the specification of the convective heat transfer between the hot combustion gases and the unignited propellant surface is developed. The technique used is an application of the pattern search technique[8] previously mentioned in this report. The coefficients are deduced by selecting the set of heat transfer coefficients at various stations within the Space Shuttle SRM's which give the best match between the prediction of the ignition transients by Caveny's method and the actual static test data. Use of the heat transfer coefficients deduced in this way forces the Caveny program to give better representation of the ignition transient for the Space Shuttle SRM's. However, there is room for much improvement. Also, the generality of the present results needs to be tested in other SRM's, where the convective heating parameters will surely exhibit differences. Hopefully, some type of semi-empirical relationship between the various SRM's is possible such that a single heat transfer relationship will apply for similar ignition techniques. Based on the present results, such efforts have been initiated by a graduate student performing research for his Ph.D. in this area.

Finally, as a separate portion of the project, a program developed by MSFC for the visual display of test data is improved and extended. This

entails adding polar plotting capability to the program and making several minor modifications to the original program.

II. THRUST IMBALANCE EVAULATION FOR THE SPACE SHUTTLE

The primary objective here is to assess the imbalance of Space Shuttle SRM pairs from static test data. It was originally planned to do this only for Space Shuttle development motors (DM's) 1 through 4, but data on the first two qualification motors (QM's) became available and are included in the final assessment.

We have previously developed a method of evaluation by which the principal known biases may be factored out of the data.[2] Such biases introduce non-random differences between individual motors of a pair which would presumably not exist in flight pairs. An example is the bias introduced in burning rate between DM-2 and 3 by adjustment of the oxidizer ground fraction.

Thus far this analysis technique has been applied only to DM-1 and DM-2.[2] With additional data now available, it is possible to perform evaluations on a number of different combinations (pairs). Results of such evaulations are compared to the thrust imbalance envelope predicted by the most recent Monte Carlo theoretical analysis.[13] This is in pursuit of the secondary objective of this task, further validation of the Monte Carlo analysis.

Imbalance Correction Program Inputs

The first evaluation is based only on the six possible combinations formed from the four DM's. In evaluating the thrust imbalance for the six pairs of Space Shuttle SRM pairs,corrections were made only in the following variables: burning rate coefficient, initial throat diameter, initial propellant bulk temperature and ignition interval. Table II-1 gives the data that formed the basis for the corrections. The method used to correct thrust versus time data for the differences in the variables, which are assumed to be non-random biases, is given in the previous report.[2] However, one modification is made in the correction approach. This is in the method of

Table II-1. Values of certain (assumed) non-random variables for Space Shuttle Development Motors

Variable	DM-1	DM-2	DM-3	DM-4
Burning rate (5" c.p. @ 625 psia, 60°F), in/sec	0.3455	0.3435	0.3635	0.3620
Initial throat dia., in.	54.418	54.429	54.427	54.416
Initial propellant bulk temperature, °F	79.5	76.0	66.6	68.3
Ignition interval, sec	0.219	0.233	0.252	0.256

computing the ignition interval correction. Rather than use the actual ignition interval, a correction is calculated based on the ratio of times required for each motor in a pair to reach 1.5 million pounds of thrust. It is felt in view of the substantial difference in the amount of igniter propellant among the first three DM's that this approach would better serve to eliminate the non-random variation in the ignition transient. In the case of the pair consisting of DM-3 and DM-4, no corrections were made for ignition differences, it being assumed that variations were random.

As noted in the previous report,[2] the correction method removes all random variation between the motors when correcting for design or condition changes. One significant design change, however, was not considered in this analysis: the increase of the insulation thickness in DM-3 and DM-4 over that in DM-1 and DM-2. This correction was not made due to the impracticality of obtaining the burning area of the SRM's near motor burnout. Because of the insulation difference, the most significant thrust imbalances are between pairs DM-1 versus DM-2 and DM-3 versus DM-4.

Thrust Imbalance Results (Development Motors)

Results of the thrust imbalance correction computer program are now given using the four Space Shuttle DM's to form six motor pair combinations. Figure 1 is a computer plot of the imbalance versus time for all six pairs obtained with no corrections. Figure 2 is a plot of the imbalance of all six pairs with the motor having the higher number motor corrected to the lower numbered motor in the pair and with the results of the Monte Carlo analysis superimposed. Figure 3 is a plot of the imbalance when DM-2 is corrected to the conditions of DM-1 and Fig. 4 is a plot of the imbalance when DM-4 is corrected to the conditions of DM-3.

Examination of Fig. 2 shows that even the results of the corrected data are well outside those results predicted by the Monte Carlo analysis of the Space Shuttle SRM's. There are several reasons for these gross discrepancies, the first of which is the lack of corrections for insulation changes. This first discrepancy results in a built-in thrust imbalance at tailoff which is much more than when motors having the same insulation design are compared as in Fig. 3 and Fig. 4.

The second discrepancy is in time of burn between the predicted results and the actual firings. A time-wise displacement results in the peak imbalance for those pairs which include DM-1 and/or 2 because the burn time used in comparing the motors of a pair is that of the longer burning motor. However, DM-3 and DM-4 are built most nearly like the final flight motors and their burnout occurred very near that predicted as can be seen by comparing Figs. 2 and 4.

A third discrepancy occurs between approximately 80 seconds and 110 seconds of burn, possibly due to a relatively small burning instability in the SRM's in this region. The only other significant discrepancy in thrust imbalance occurs between the ignition transient and approximately 30 seconds of burn. There is no ready explanation for this discrepancy; however, it is less pronounced in Fig. 4 for DM-3 and DM-4.

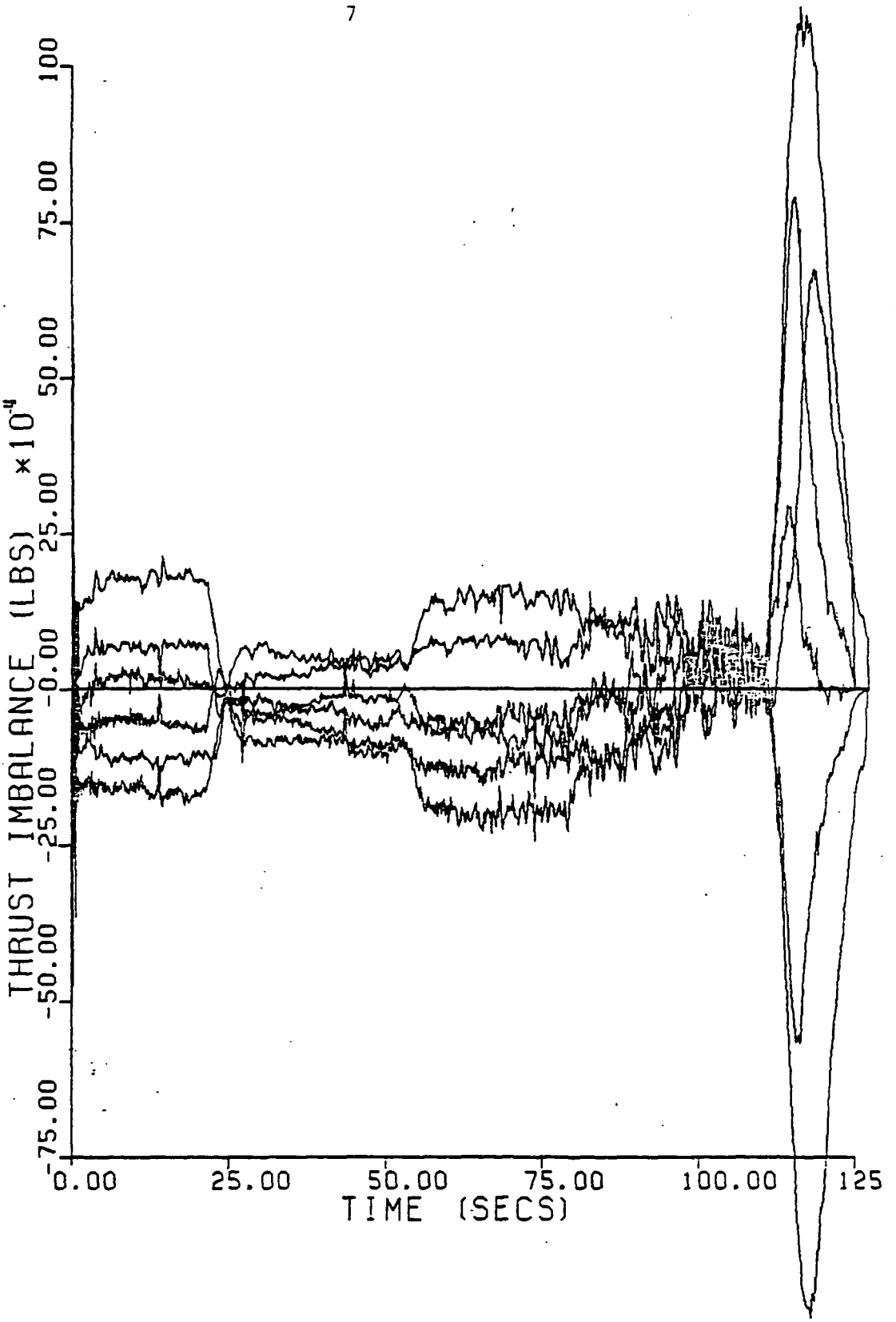

Fig. II-1. Uncorrected thrust imbalance versus time for six pairs of SRM's based on the first four Space Shuttle SRM's (DM-1 through 4).

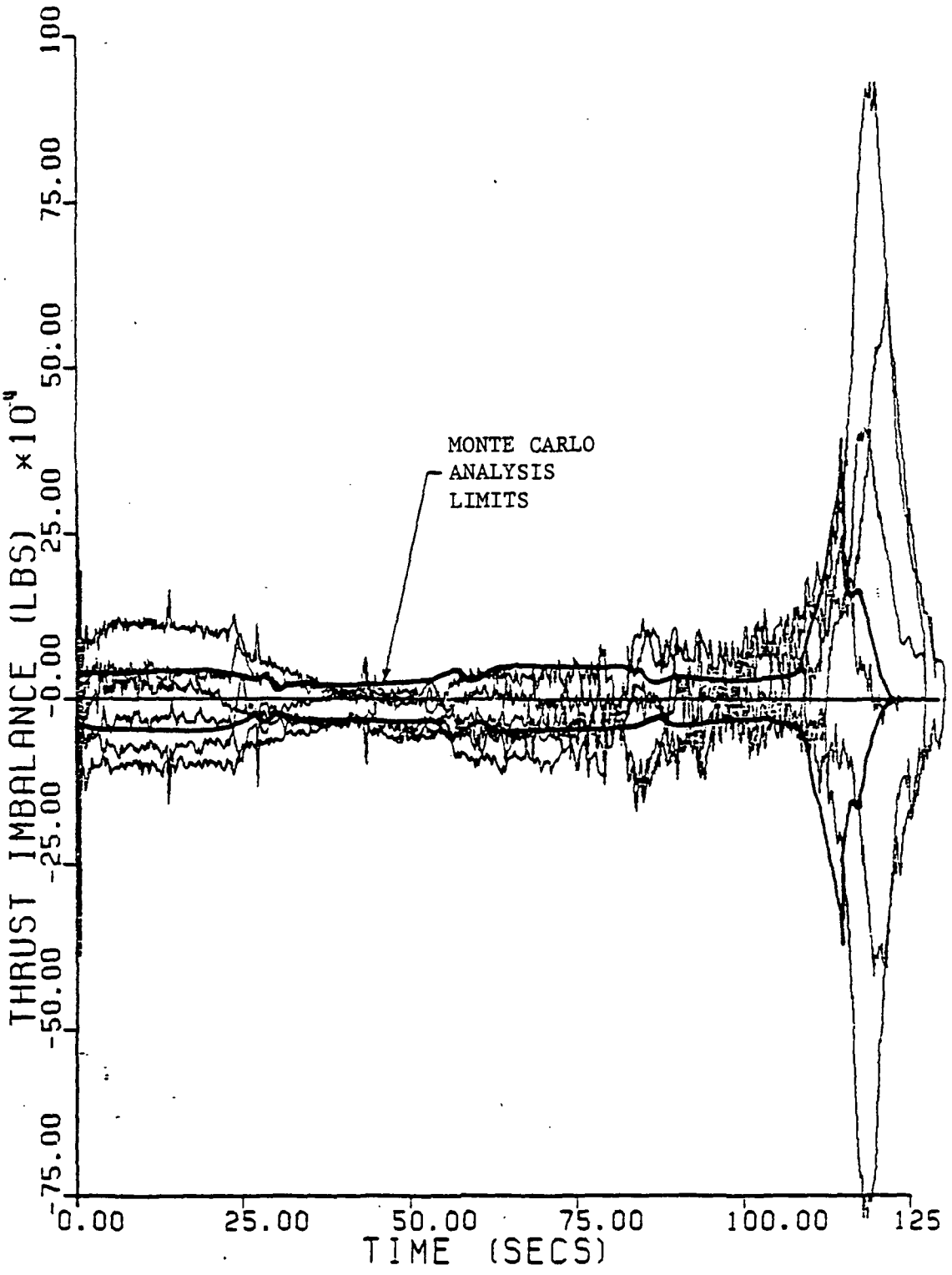

Fig. II-2. Corrected thrust imbalance versus time for six pairs of Space Shuttle SRM's based on static test data for the four development SRM's.

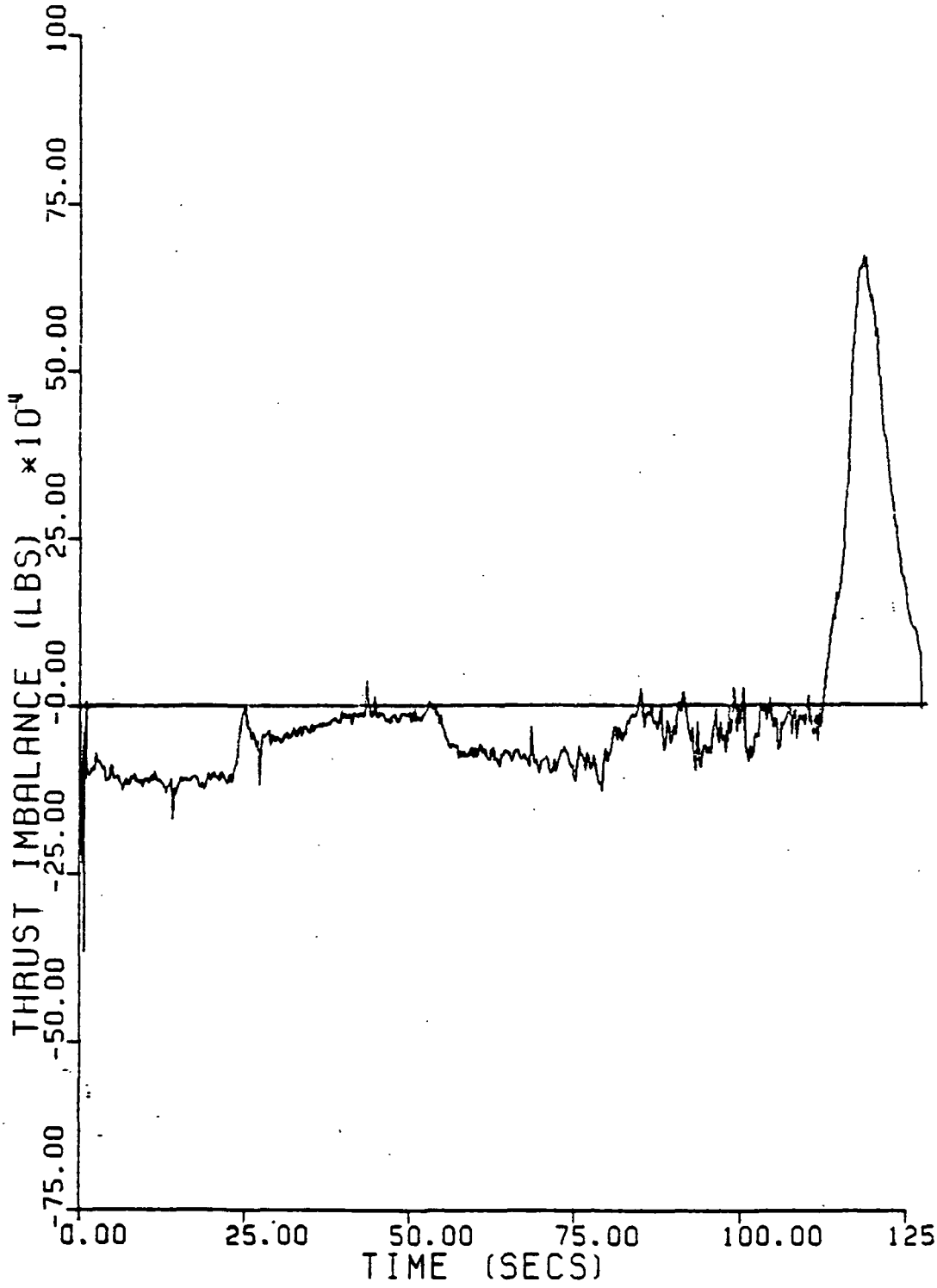

Fig. II-3. Corrected thrust imbalance versus time for the first two Space Shuttle SRM's (DM-1 and 2).

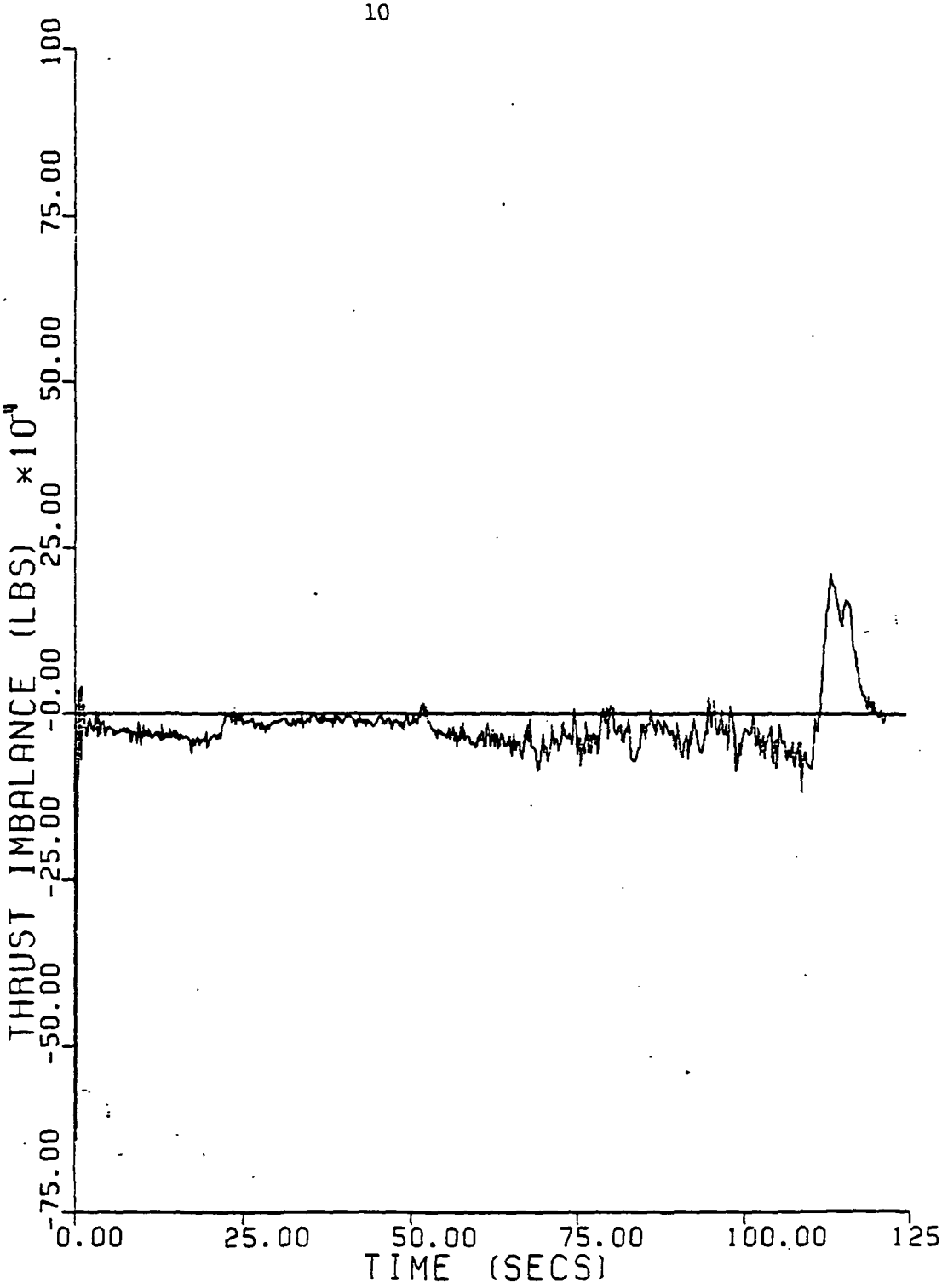

Fig. II-4. Corrected thrust imbalance versus time for the third and fourth Space Shuttle SRM's (DM-3 and 4).

The maximum thrust imbalance limits as recently assessed by a Monte Carlo analysis of the Space Shuttle SRM's, calculated without regard to propellant temperature gradients and without regard for the time at which the maximum imbalance occurs are ±405,500 lbf.[13] The Monte Carlo analysis excludes the ignition transient. The limit as assessed from the worst case for the six pairs studied, DM-1 and corrected DM-3, is 926,000 lbf. However, because of insulation differences, which lead to uncorrected discrepancies in geometry between these two motors, this is not a good assessment of thrust imbalance to be expected in production pairs. The two pairs of motors which are built most nearly alike, DM-1 and DM-2 and the pair DM-3 and DM-4, have limits of 419,000 lbf. and 246,000 lbf, respectively. The first value is 103% of the limit while the second value is only 61% of the limit. Because DM-3 and DM-4 are built most nearly like a production motor of the four motors compared here, the pair having the 61% difference between the limits is probably the only one truly representative of the family of production pairs.

Thrust Imbalance (Qualification Motors)

The acquisition of data on QM-1 and 2 late in the study of thrust imbalance make possible a more complete investigation of the thrust imbalance to be expected in flight vehicles. For this purpose, the behavior of six pairs composed from DM-3 and 4 and QM-1 and 2 are analyzed. All differences between SRM's of a pair are considered random in this case except the propellant bulk temperature for which corrections are made. (The bulk temperatures for QM-1 and 2 are 72.0 °F and 73.4 °F, respectively. See Table II-1 for DM-3 and 4 temperatures.)

Results of the analysis are given in Fig. II-5. The Monte Carlo theoretical limits are also superimposed on the test results. Figure II-5 shows the various pairs exhibit much lower thrust imbalance than that of the pairs composed from the development motors. It should be kept in mind that this is in spite of the fact that the only correction made in the data from which Fig. II-5 is obtained is in the propellant bulk temperature. It is also notable that the last results are generally consistent with the Monte Carlo limits predicted.

Finally, as a matter of special interest, the thrust imbalance between QM-1 and QM-2 is depicted separately in Fig. II-6, with a maximum thrust imbalance of 211,900 lbf or 52% of the limit.

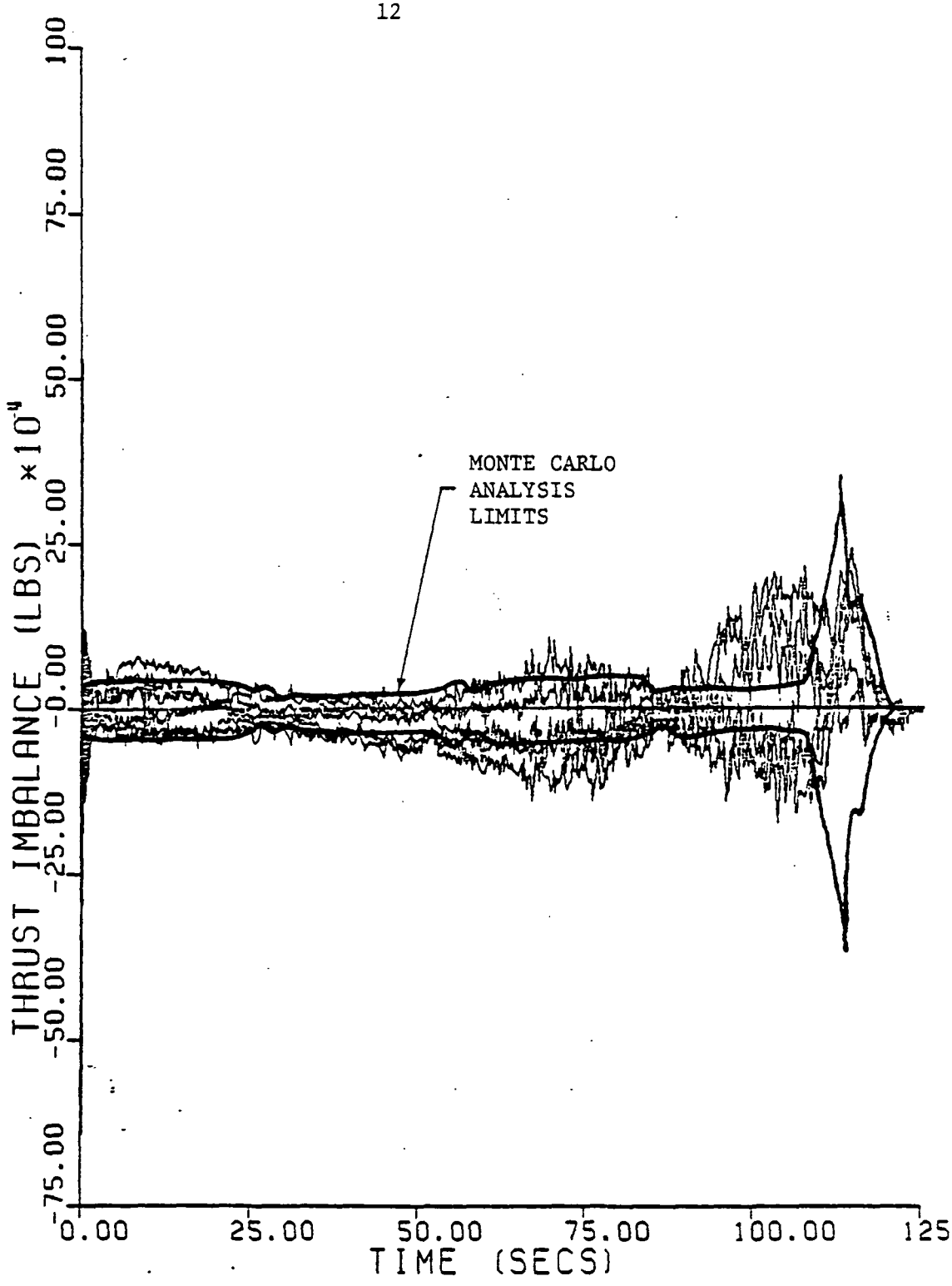

Fig. II-5. Thrust imbalance versus time corrected for propellant bulk temperature differences for six pairs of Space Shuttle SRM's based on static test data for DM-3 and 4 and QM-1 and 2.

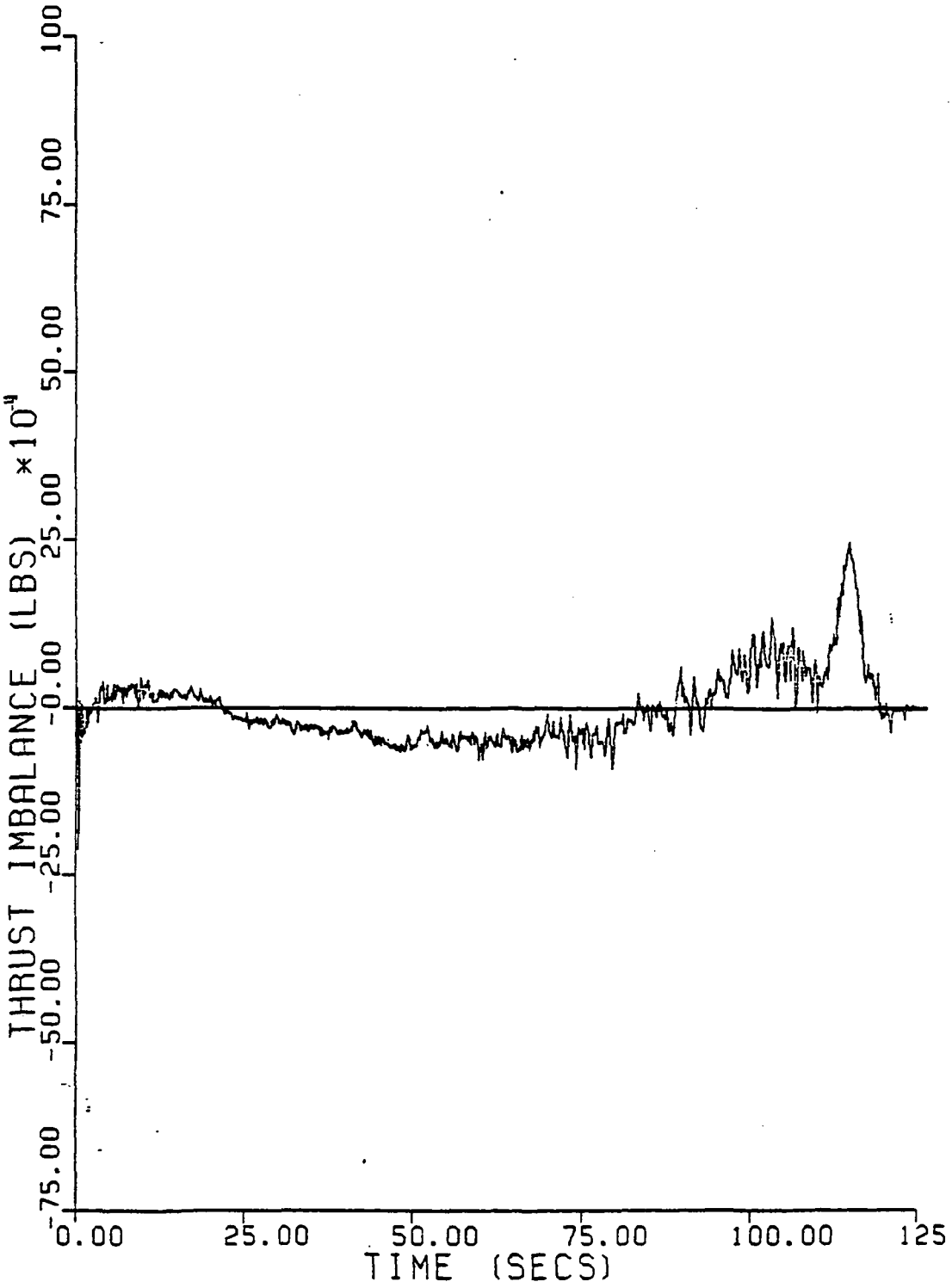

Fig. II-6. Thrust imbalance versus time corrected for the propellant bulk temperature difference for Space Shuttle QM-1 and QM-2.

III. PROPELLANT DEFORMATION AND BURNING RATE MODELS

A good mathematical model of the internal ballistics performance of single SRM's is essential to the design process. Likewise, it is necessary for theoretical prediction of thrust imbalance characteristics. To achieve the goal of a superior model previous studies were conducted of the ballistic effects of propellant deformation[2,4] and of propellant burning rate characteristics.[2,3] Good results were achieved but the burning rate relationship lacks generality.

The relationship assumed was largely an empirical one and did not recognize the apparent effects of motor configuration on the burning rate except as dictated by its influence on the mass flow rate per unit area. On the other hand, configuration appears to play an additional role in the establishment of the burning rate. This is evidenced, for example, by the need to adjust the erosive burning constant c_4 between the DM-1 and its associated ballistic test motors in order to achieve good predictions of the performances of both.[2]

Attempts to better the burning rate relationship by including simple factors which account for the effect of configuration and improve the generality of the relationship are now discussed. Throughout the study, evaluations are made with and without the effects of grain deformation taken into account in order to validate further the importance of this phenomenon. The results obtained are quite satisfactory in that a refined empirical burning rate model is developed which uses a single equation to yield excellent predictions of 5 SRM's of very different configuration. All of these SRM's employ PBAN type propellants with ammonium perchlorate oxidizer and 16 to 20% aluminum except one which uses carboxyl terminated butadiene binder. The only non-calculated parameters in the burning rate equations that are changed for the different SRM's are the zero crossflow velocity burning rate coefficient and exponent. The results, in general, confirm the importance of grain deformation.

It is noteworthy that the development of this new internal ballistics model, which is basically a modification of the simplified design analysis program[10,11] makes practical the development of the program for application of an optimization technique to SRM design which is presented in Section IV.

Improvement of Modified Flame Height Burning Rate Model

The original modified flame height burning rate equation used to calculate the burning rate r at the point of maximum flow Mach number is:[3]

$$1/r = 1/r_o - c_4 (GL_{ref}/L)^{0.5} (1-P_{cr}/P) \qquad \text{(III-1)}$$

While good results were obtained in predicting the performance of a number of SRM's using Eq. III-1 and the propellant deformation relationships in the simplified design analysis program, it was found that the values of the arbitrary constants c_4 and/or P_{cr} had to be changed radically for different SRM's. This lack of generality was especially pronounced in the comparison of Space Shuttle SRM calculations with those for the associated 5-in. dia. circular perforated (c.p.) ballistic test motor which uses the identical propellant.

In an effort to improve this situation, an investigation was subsequently conducted to effect an improvement by use of a variable P_{cr}.[2] The effort involved mainly a study of the Space Shuttle SRM and its associated ballistic test motors. Various trials were made with linear relationships between P_{cr} in Eq. III-1 and M_n, the maximum flow Mach number. Best results were obtained with

$$P_{cr} = - 537\ M_n + 631 \qquad \text{(III-2)}$$

With this last relation an excellent result was obtained for the 5-in. dia. motor and good results for the Space Shuttle SRM with the same value of c_4.

In the present research the generality of Eq. III-2 was tested in a number of SRM's with poor results. Effort was then directed toward improving the relationship for P_{cr}. Expressions tested included second order polynominals in M_n and various functions of burning rate and grain length. While a number of these gave good results in several of the different SRM predictions, they failed to adequately represent the apparent behavior in one or more of the other SRM's. The SRM's whose performances were evaluated in this study were: 1) the Space Shuttle SRM, 2) the Space Shuttle 5-in. dia. ballistic test motor, 3) the TU-455.02, 4) the Castor TX354-5 and 5) the Titan IIIC (UA 1205). The propellant formulations for these motors are given in Table III-1.

Table III-1. Propellant formulations.

SRM	Designation	Aluminum %	Amonium Perchlorate %	Binder System %	Iron Oxide %	Curing Agent %
DM-1 and 5-in. dia. (Space Shuttle)	TP-H1148 (PBAN)	16.00	69.81	12.04	0.19	1.96
TU-455.02	TP-H8163 (PBAN)	16.00	69	12	1	2
TX354-5	TP-H7036 (Carboxyl terminated butadiene)	20.0	68.0	12	-	†
UA 1205 (Titan IIIC/D)	UTP 3001 (PBAN)	16.12	67.51	13.28	0.25	2.84

†Curing agent and plastizer are included in binder.

Attempts were then made to improve the ballistic performance predictions by permitting c_4 to vary as various functions of burning rate and motor geometry along with variations in P_{cr}. After hundreds of different evaluations, good general results were obtained with the following expression giving the burning rate at the position of maximum flow Mach number:

$$1/r = 1/r_o - c_4 \left(GL/L_{ref}\right)^{0.5}(1-P_{cr}/P) \qquad \text{(III-3)}$$

where

$$c_4 = 18.5\ (D_p/L)^{0.8} \qquad \text{(III-4)}$$

and

$$P_{cr} = 3755\ r^{0.2}\ (D^*/L)^{0.7} \qquad \text{(III-5)}$$

One important additional modification was made in the basic design analysis program,[10,11] along with the modifications for grain deformation effects.[3,4] This was in the method for calculation of P_h, the pressure at the head end of the propellant. One of the assumptions made in the earlier work which greatly simplifies the program is that this pressure can be calculated from the frictionless one-dimensional momentum equation for a constant cross-sectional area port. In applying this momentum equation to a tapered grain, the (constant) area assumed was taken as the arithmetic average of the front and aft end (maximum Mach number position) areas. This resulted in a rather consistent underestimation of the head end pressure. After a rather detailed investigation in the present work, it was found that much better results were obtained if the port area was taken as the smaller of the aft and head end areas at each instant of time. During this investigation, trials were also made on a modified momentum equation wherein the earlier calculation was multiplied by various powers of L/D in order to establish the possible importance of frictional effects. Results were generally unsatisfactory.

The Ballistic Performance Equation

Final results for the 5 SRM's are presented in the pressure versus time traces given on Figs. III-1 through III-5. Predicted results are given with and without grain deformation effects and compared with actual performance data.

Two special and separate modifications of the basic analysis are made in the calculations for the 5-in. dia. motors and the UA 1205. In the case of the 5-in. dia. motors, the one modification is in the method of averaging the head and aft end burning rates for use in calculating the rate of mass of propellant gases generated. In previous evaluations involving the 5-in. dia. motors, it was found beneficial to restore the arithmetic averaging of the fore and aft burning rates used in the internal ballistic model.[2] In other motors, a somewhat arbitrary correction technique was used

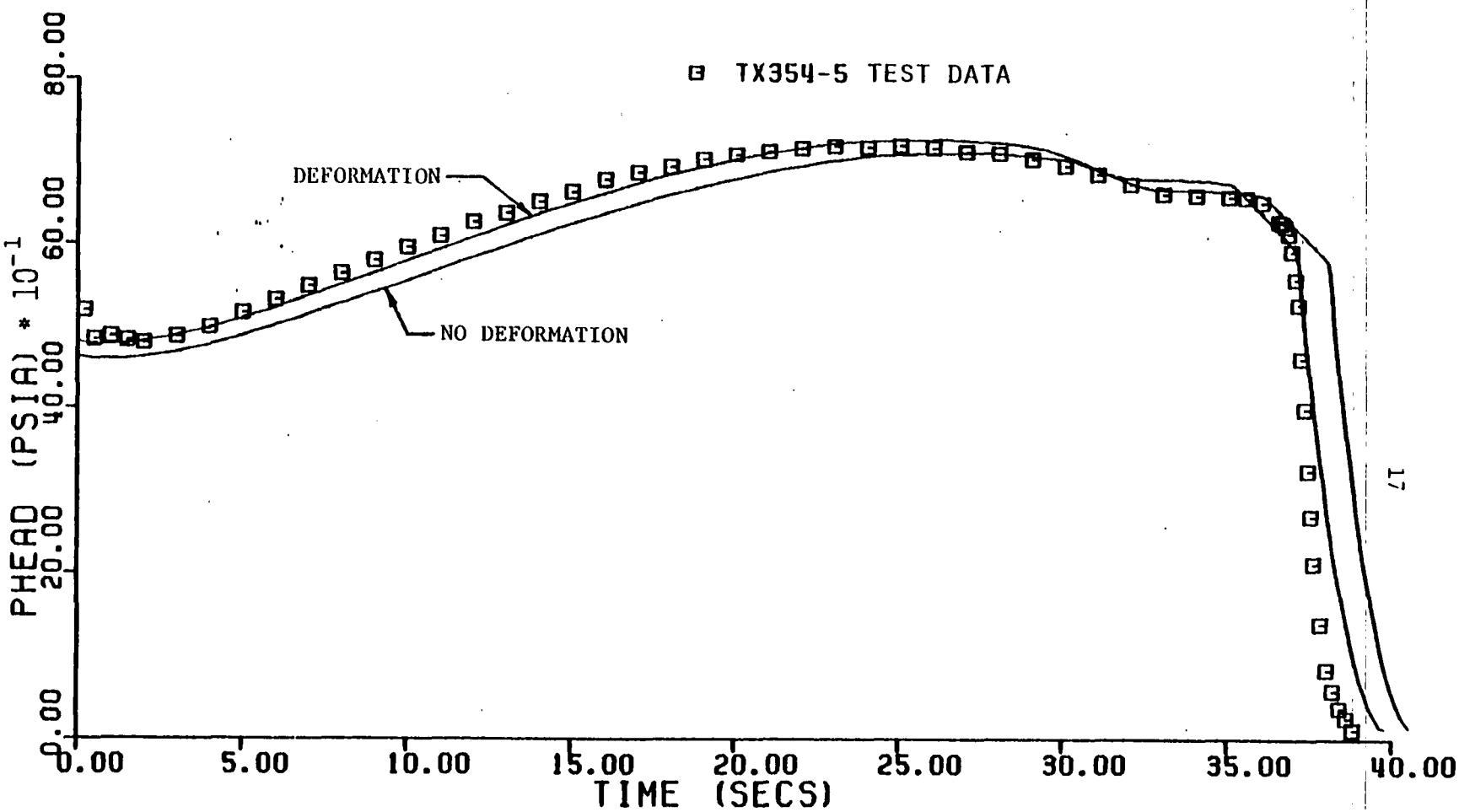

Fig. III-1. Comparison of test data for the Castor TX354-5 with theoretical performance calculations.

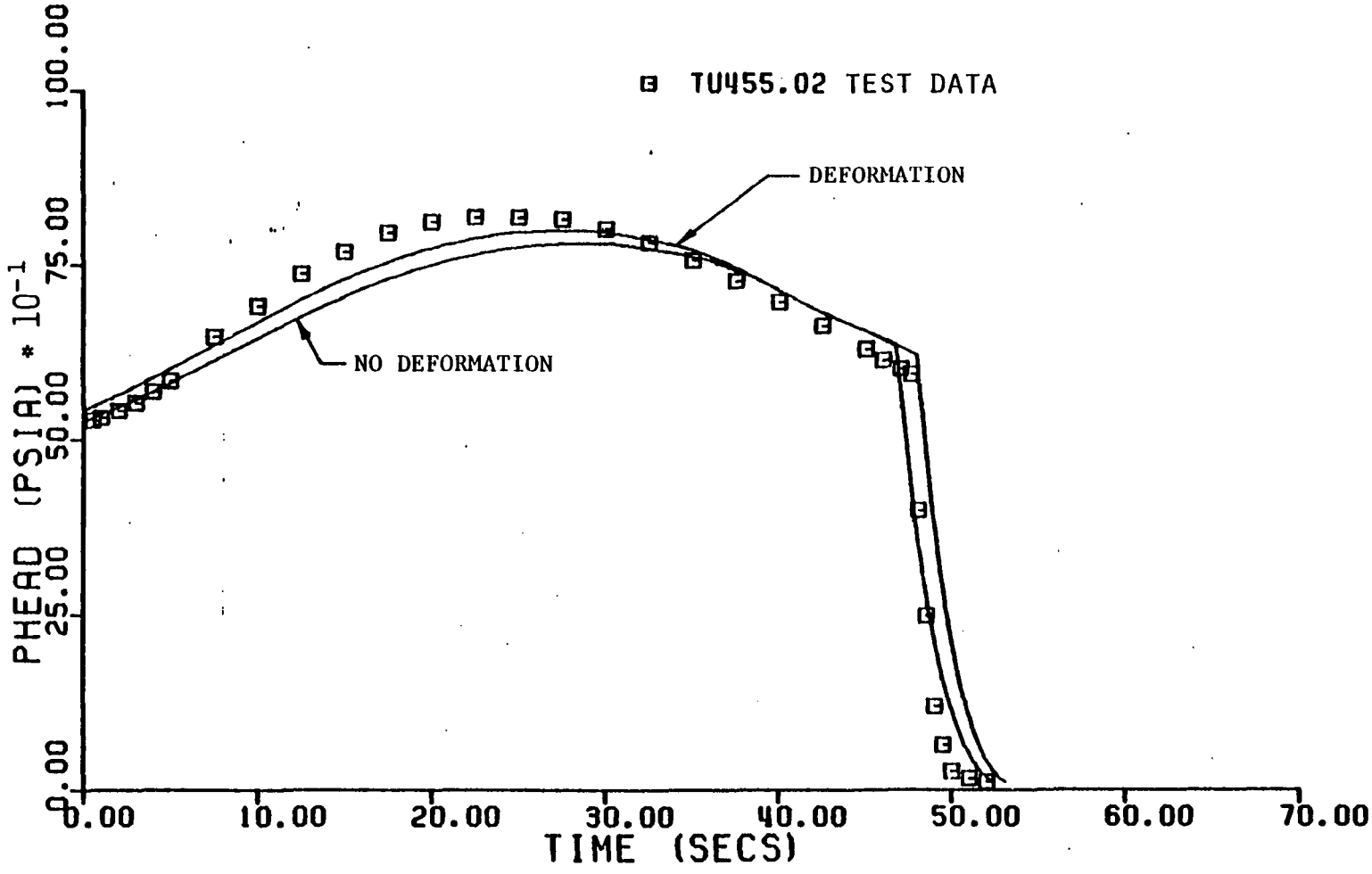

Fig. III-2. Comparison of test data for the TU-455.02 with theoretical performance calculations.

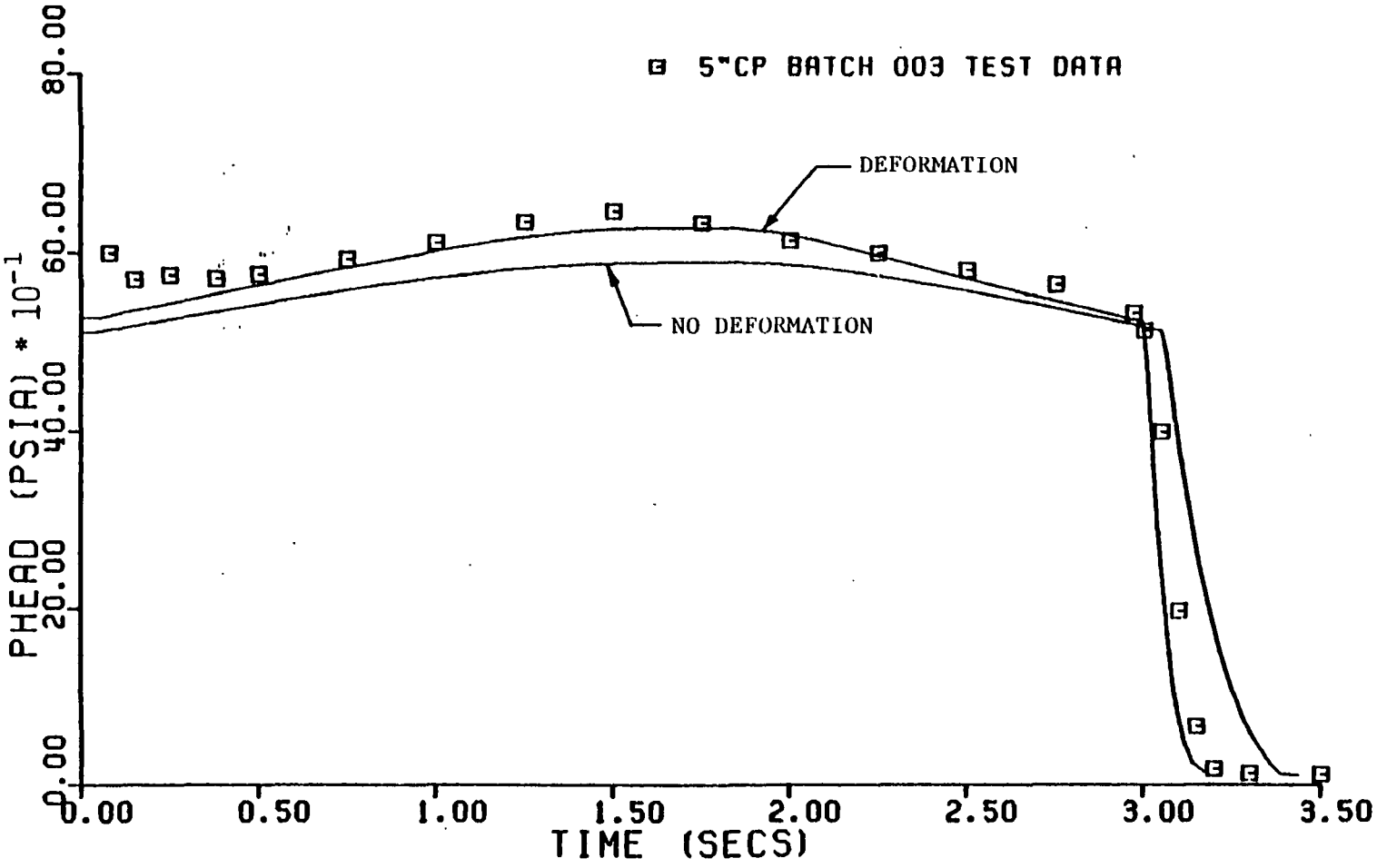

Fig. III-3. Comparison of test data on Space Shuttle 5-in. dia. ballistic test motors for DM-2 with theoretical performance calculations.

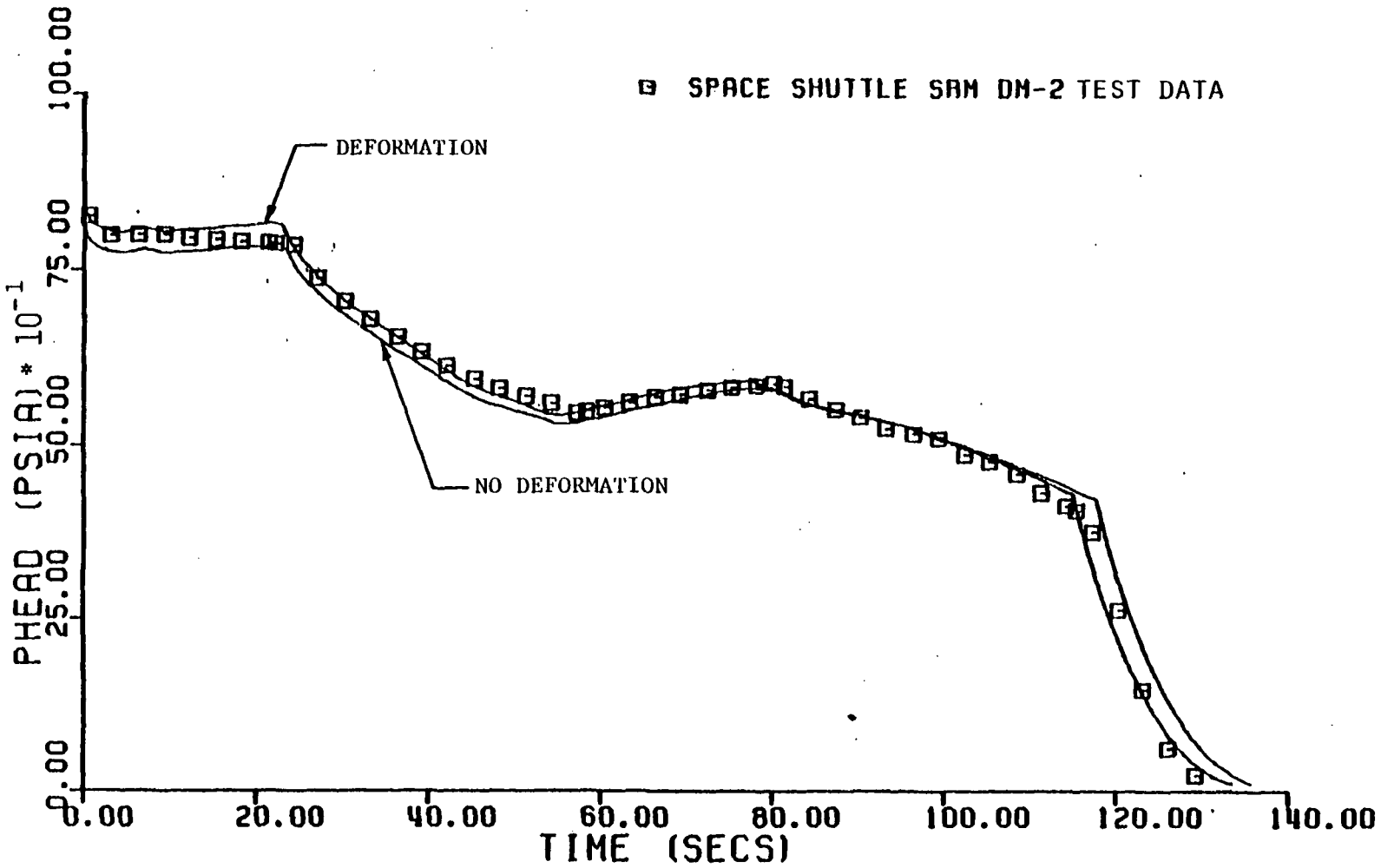

Fig. III-4. Comparison of test data on Space Shuttle DM-2 SRM with theoretical performance calculations.

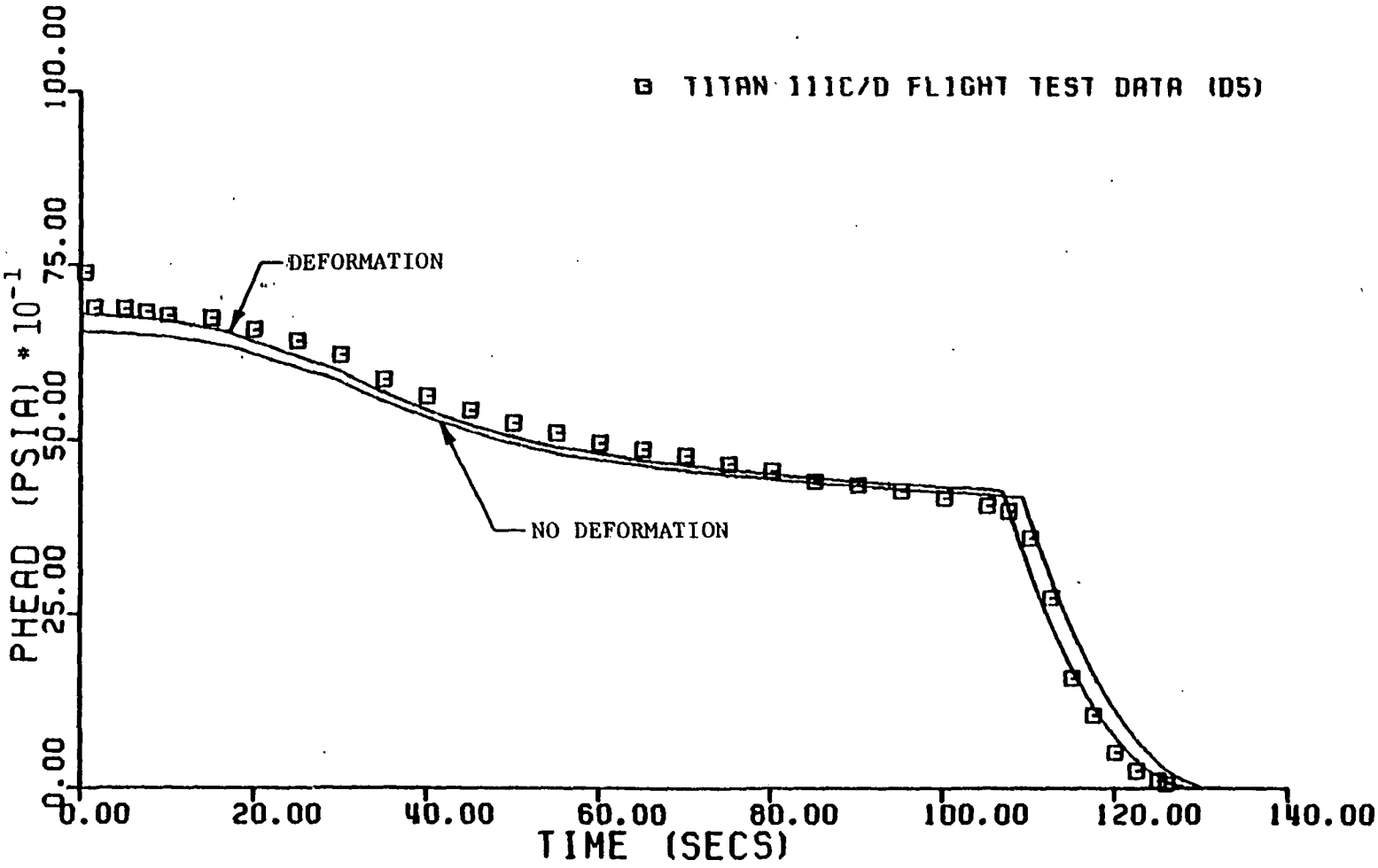

Fig. III-5. Comparison of test data on Titan III C/D, UA1205, with theoretical performance calculations using a modified grain taper representation.

to gradually reduce the influence of the aft end rate on the "average" rate.[3] The unique treatment of the 5-in. dia. motors is retained in the present analysis. For the Space Shuttle DM-2 evaluation, either approach yields essentially the same results since the head and aft end rates near tailoff are quite similar. For the other SRM's significantly better results are obtained with the earlier approach[3] and this is used in all the other evaluations. The results for the 5-in. dia. motors with the alternative technique are given on Fig. III-6. It appears from the analysis that in the regime of extremely low cross-flow velocities and high critical pressures with respect to the actual pressure, such as occurs as tailoff is approached in the 5-in. dia. motor, the linear average burning rate is more applicable than the nonlinear average as used in the simplified design program.

For the UA 1205, the special consideration given is in the assignment of z_o, the initial difference between web thickness at the head and nozzle ends of the controlling length of the grain. Each of the five center segments in the UA1205 are identical. It is, however, necessary to represent the taper of these segments in the design analysis program by a single continuous taper fixed by the assignment of z_o. In general, the z_o that has been used is that of a single segment; i.e., 5.0 inches for the UA 1205. Because the aft end burns faster than the head end of the propellant, this results in a somewhat slower tailoff rate in the theoretical performance than actually occurs. To obtain Fig. III-5, the z_o for the UA 1205 was arbitrarily reduced to 4.0. The result with $z_o = 5.0$ is presented in Fig. III-7 which shows that the reduced z_o betters the prediction. Further improvement may be possible by further reduction of z_o. Also, the Space Shuttle SRM results could probably be improved somewhat by a similar treatment since two identical tapered sections are used in that SRM.

Discussion

From the ballistic performance evaluations it is seen that, in general, better results are obtained when the propellant deformation is taken into account. However, this conclusion is not as clear for the Space Shuttle DM-2 as for the other motors. It appears deformation effects may be overestimated somewhat in the Space Shuttle. One possible explanation is that the value of the propellant Poisson's ratio used in the Space Shuttle analysis (0.499) may be inaccurate, and the results are quite sensitive to this property. The DM-2 prediction would benefit from a slightly higher Poisson ratio. However, results for the 5-in. dia. motor would be poorer with a higher Poisson's ratio. Another possible explanation for the problem with the DM-2 results might be the effect of the star portion of the grain which is not taken into account in the analysis.[3]

The new modified flame height burning rate model is presently applicable to only one general type of propellant and is largely empirical. Also, its adequacy has only been demonstrated with the simplified design analysis program. Undoubtedly, the assumptions made in the program introduce model biases when the constants in the burning rate relation are

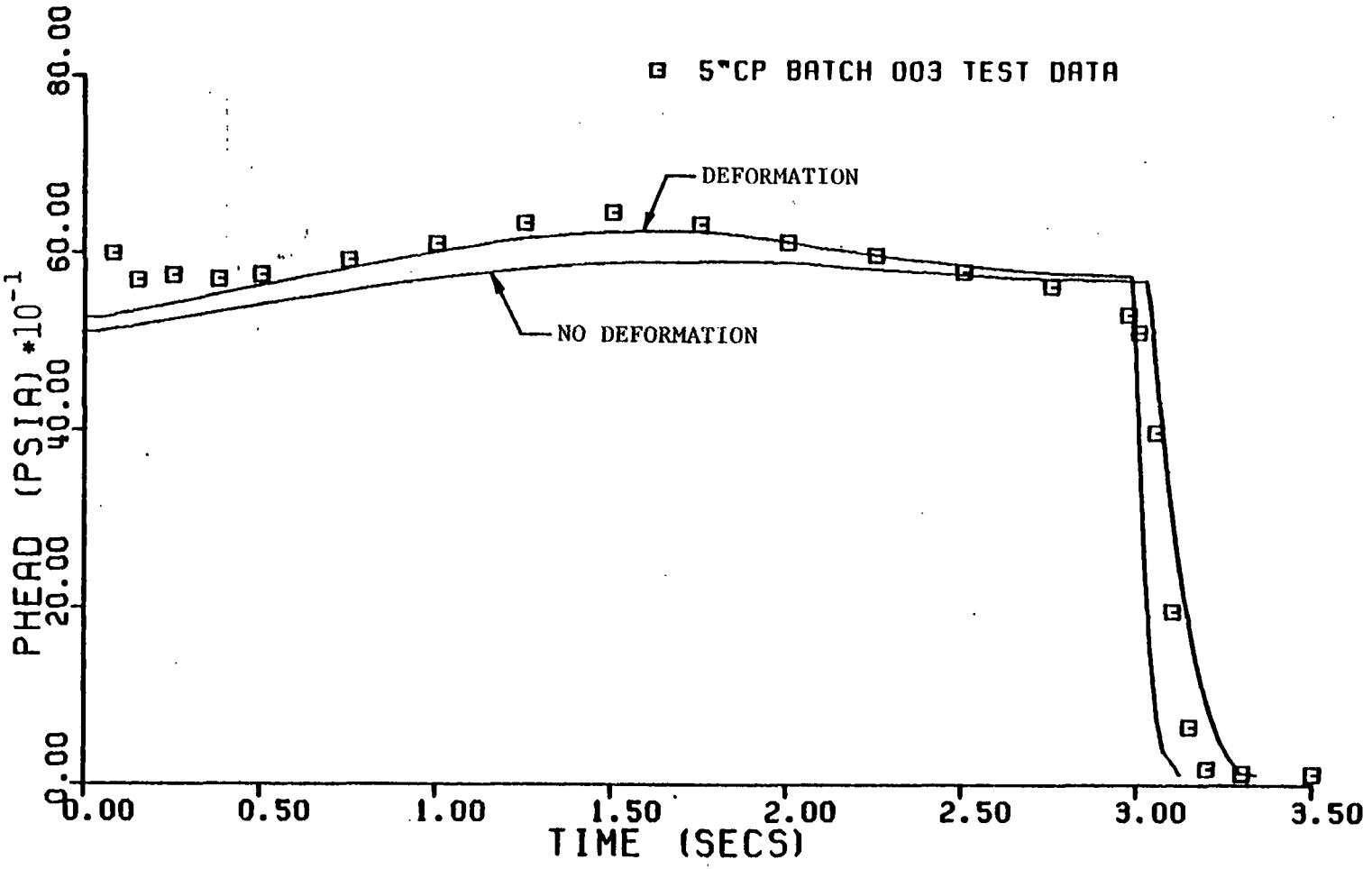

Fig. III-6. Comparison of test data in Space Shuttle 5-in. dia. ballistic test motors for DM-2 with theoretical performance calculations based on a non-linear length varying burning rate.

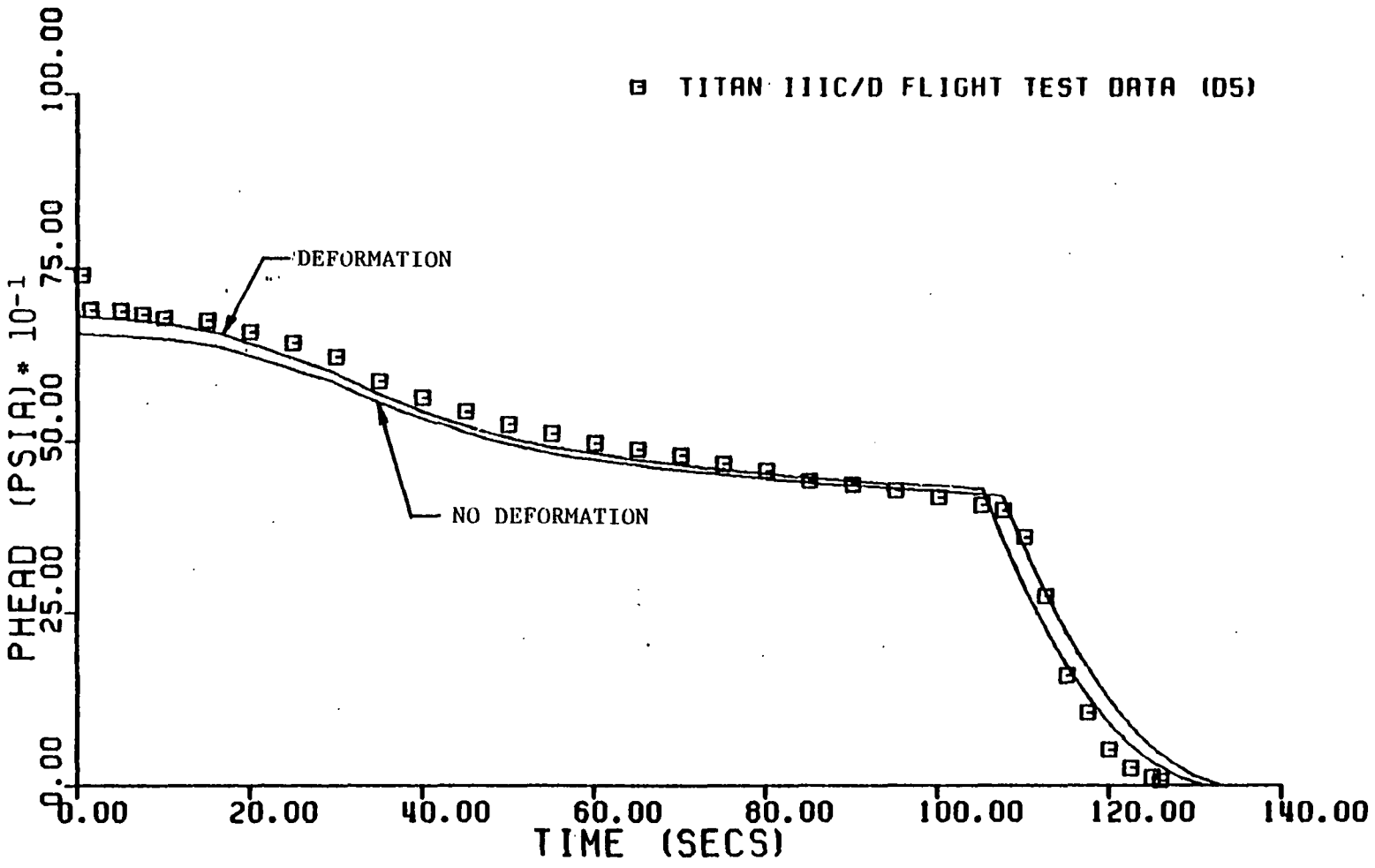

Fig. III-7. Comparison of test data on Titan III C/D, UA 1205, with theoretical performance calculations using actual grain taper.

determined. Nevertheless, the generality of the results is quite remarkable. The model fits the behavior of a number of SRM's with widely different configurations over broad ranges of pressures, crossflow velocities and burning rates.

The form of the burning rate relations (Eqs. III-3 through 5) contains the following features which appear to be well established as general trends:[14] 1) The erosion effect is more pronounced at lower rates (lower P_{cr}) for positive erosion, 2) Negative erosion is possible, and 3) The erosion threshold is pressure sensitive. The parameter GL/L_{ref} in Eq. III-3 is a combined Reynolds number and Nusselt number effect discussed in previous work.[3] The D_p/L factor in Eq. III-4 is reasonably attributable to boundary layer buildup phenomena. The presence of r in Eq. III-5 is necessary because of the effect of blowing on convective heat transfer. A satisfactory specific explanation of the D^*/L factor in Eq. III-5 has not been found, but it is likely indicative of a much more complicated effect of motor configuration on heat transfer feedback to the propellant surface than is described by the other factors in Eq. III-5.

The demonstration of success with the new burning rate model is impressive enough to warrant additional investigation. The empirical model should be tested in other SRM's which use both similar and different propellants. Also, although the specific constants in the burning rate relations were the result of extensive analysis, the investigation cannot be termed exhaustive. It is possible that alternative sets of values for these constants may be established that yield even better results. Likewise, the form of the equations might possibly be improved. Finally, additional efforts should be made to reconcile erosive burning theory with these results.

IV. SOLID ROCKET DESIGN AND OPTIMIZATION PROGRAM

Woltosz[9] has demonstrated the application of a mathematical optimization technique to the selection of SRM design parameters that meet certain design goals. In particular, for an SRM of the Space Shuttle size class he shows how a set of 5 critical design dimensions are determined which, for a specified minimum ideal vehicle velocity, maximize the total impulse-to-motor weight ratio without exceeding a specified maximum allowable web fraction. For this purpose, he develops a computer program which uses the direct pattern search optimization technique of Hooke and Jeeves[8] and the simplified design analysis program of the present writer.[10,11]

In previous MSFC sponsored research,[2,7] the same pattern search technique is applied to minimize the difference between certain main motor performance characteristics desired and those calculated using a simplified mathematical model[11,15] of the ignition transient. For example, the set of 5 igniter design characteristics is selected which minimizes the summation of the squares of the differences between the desired and computed SRM thrust values during ignition.[2]

In the present work, a practical computer program similar to the ignition optimization is demonstrated which will match overall main motor desired performance, i.e., a specified thrust time trace, to calculate performance by optimum determination of main motor design parameters. Because of the large number of complete ballistic analyses necessary in the search for the best match of desired and calculated values, the simplified design analysis program[10,11] is used for the internal ballistics calculations.

The computer program of Woltosz is modified to include the new optimization criterion while retaining the two separate criteria of the original program as options. In addition, extensive revisions and additions are made to: 1) improve the pattern search technique for the purpose of reducing computer operating time, 2) provide a more accurate ballistic model so that the search will accurately converge, 3) specify more adequately the design constraints that assure a set of final design parameters that describe an SRM of practical design, and 4) include additional design variables. Details of these modifications are discussed next. Finally, a demonstration of the program is presented with 10 design parameters as variables. A familiarity of the reader with the simplified design analysis program[10,11] and optimization program of Woltosz[9] is assumed. Alternatively, a listing of the revised optimization program which has been liberally annotated will provide the essential user information.

General Description of the Program

The new optimization program is named "Solid Rocket Motor Design and Optimization Program (SRMDOP)." The program contains the following routines: The MAIN establishes the design variables which are to be varied during the search for the optimum. Any number of the 15 geometric variables which are defined by Fig. IV-1 may be so treated. The burning rate coefficient Al may be used as an additional variable. Storage space is reserved in the

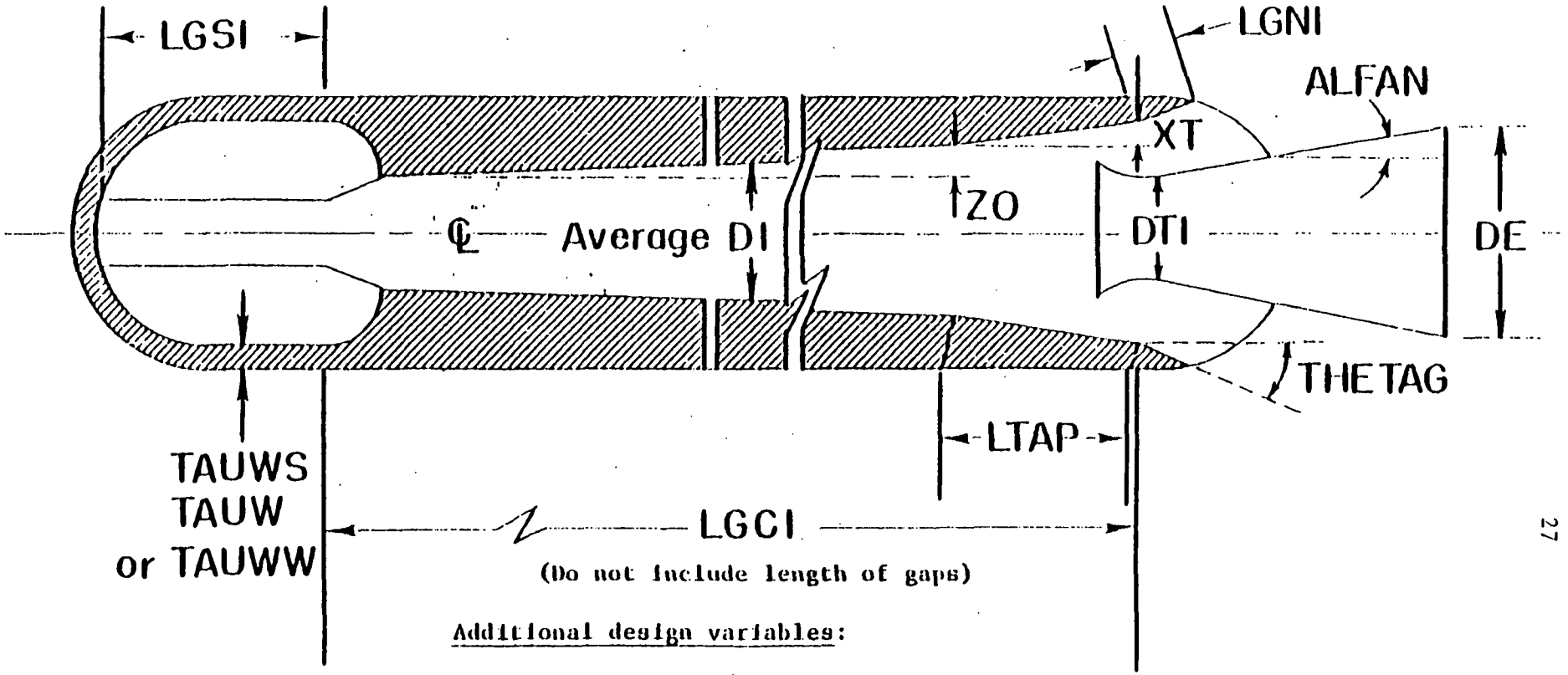

Fig. IV-1. Variable design parameters to be fixed by SRMDOP. The variables TAUWS, TAUW and TAUWW are the web thicknesses for a standard star, truncated star or wagon wheel configuration, respectively.[10] Special burning geometry caused, for example, by a head end web of a star grain and/or a transition section between a star and a c.p. grain are treated by an iterative procedure making use of tables of positive and/or negative values of burning surface versus distance burned.

program to facilitate modification to accommodate up to nine more variables. The MAIN also provides the input controls: the parameters which specify the constraints on the variables, the amount of data provided as output, and the step size to be used during the search.

Subroutine PATSH conducts the pattern search following the method of Hooke and Jeeves[8] as adapted by Woltosz[9] from a program developed by D. E. Whitney which is now modified as discussed later.

Subroutines BURNIT, AREAS and OUTPUT contain the elements of the simplified design analysis program[10,11] as modified by Woltosz and subsequently by the present investigators.

Upgrading of the internal ballistics computer program is essential to the new optimization program. If the ballistics of the SRM cannot be properly modeled, the program, in an attempt to match the required thrust-time trace, will force the variables to erroneous values. If the SRM is then built to these specifications, its actual performance will not conform to that desired.

Major improvements have been made in the performance calculations obtainable from the simplified design analysis by including the modified flame height burning rate model and the grain deformation analysis discussed in section III of this report. Another very important improvement is made by restoring, to the simplified design analysis program, the option of representing special propellant burning geometry through the input of tabular values of burning surface versus distance burned. This permits the program to treat, for example, a star grain intersecting a curved closure or to treat a transition section between star and circular perforated (c.p.) grain sections. However, in the use of this option, it may be necessary to approach the design in stages since the surface versus distance burned associated with these special sections cannot be determined until the final design parameters are fixed. In the first stage, the special surface versus distance burned trace would be separately determined based on the starting (input) configuration. Once the program has determined the optimum set of variables based on this input, a new burning surface trace can be determined and used as input to redetermine the optimum variables. A few iterations of this type should suffice to fix an accurate solution. Of course, if the variables used do not affect the geometry of the special sections, iteration is unnecessary.

Woltosz[9] uses relatively few constraints on his input variables. He, however, constrains DE to be greater than twice DTI and less than the case diameter, ALFAN to be less than and greater than specified values, and the web fraction (controlled by DI) to be within specified limits. Also, a fixed lower limit (0.5 inches) is set for FILL. Other lengths and angles are required to be > 0. Such constraints are required to prevent the program from selecting impractical or absurd values for the variable design parameters. In the present program, the number of constraints are modified and increased in number. The upper limit on DE is now arbitrary. The range of initial throat diameter DTI is now set by upper and lower limits

on the throat-to-port area ratio. The lower limit on FILL is now an input. Upper limits are also now specified for LTAP, XT, ZO, THETAG, LGCI, LGNI, THETAG, FILL, TAUS and TAUWS. These latter upper limits are established within the program. For examples, LTAP must meet the internal limit of being less than one-half the estimated total grain length L and XT must be less than 10% of LTAP.

Two new design optimization variables have been added to the program. These are TAUWW, the web thickness of a wagon-wheel grain or grain segment, and A1, the propellant burning rate coefficient. Both of these new variables are constrained by specified arbitrary upper and lower limits.

As in the original program, constraints are enforced by the use of penalty functions which by adding a relatively large number to the objective function (function to optimized) force the search away from conditions which cause the constraints to be violated. The value of the penalty is assigned in proportion to the square of the amount by which the constraint is violated. To avoid difficulties with possible mathematical discrepancies that could be encountered when a constraint is violated, in addition to assigning a penalty function, the value of the variable is set equal to the constraining value whenever a constraint is violated.

As previously indicated, there are three options, any one of which may be selected by the user as a single optimization criterion. The two criteria used by Woltosz are retained: 1) maximize the ratio of total impulse to motor weight, and 2) minimize motor weight. Each of these criteria are subject to the side condition enforced by the use of a penalty function, that a specified minimum ideal vehicle velocity be obtained. Here the ideal velocity is that obtainable at burnout with no payload, drag, nor gravity. Such optimization is of some value in design when little or nothing is known of the mission for the rocket. Also, the program could easily be modified to include payload, drag and gravity considerations in the constraining equation.

In the new program, a third option has been added to force the search to select a set of design parameters which give the predicted thrust-time trace which most nearly matches a desired thrust-time trace. The desired trace is specified by input of a discrete number of thrust values and their corresponding time points. The program calculates the thrust values at the same time points for each set of design parameters assigned during the search. The objective function Φ is then given by the following equation:

$$\Phi = \sum_i f(\Delta F_i)^2 + \sum_j P_j \qquad \text{(IV-1)}$$

Here ΔF_i is the difference between the desired and predicted thrust at the ith time point and f is an arbitrary weighting factor to be assigned to each thrust-time point. The penalty function for the jth constraint is P_j, and is zero if the constraint is not violated but otherwise a large positive

number multiplied by the square of the amount by which the constraint is violated. The minimization of Φ thus leads to the condition where all constraints are satisfied ($\sum_j P_j=0$) and $\sum_i f(\Delta F_i)^2$ is a minimum. This in turn yields the "best match" between predicted and desired performance.

Two major modifications of the original pattern search technique[9] are incorporated in the new program. In the early part of the present investigation it was found that excessive time was being consumed in the program in both exploratory and pattern moves[2,8,9] involving only variables to which the performance (thrust vs. time) was only slightly sensitive. The search would try to attain the minimum Φ by repeated adjustment of these variables at the same step size δ while holding the other variables constant, because the effects of these variables were so sensitive that at the larger step sizes they produced large values of Φ. The solution is to disregard the changes produced by the variables which affect performance only slightly and to proceed directly to the reduction of δ. Of course at reduced step size the sensitivity of all variables becomes important. The overall problem is solved in the program by rejecting moves for which

$$\Delta\Phi < 0.05\ \Phi\ \delta^{1.5} \qquad \text{(IV-2)}$$

Here $\Delta\Phi$ is the change in Φ during a move and $\delta=1$ corresponds to 5% in the variable for which a change of less than 5% in Φ would be rejected. The exponent of δ was fixed by trial and error to provide an efficient search which permits the variables with small effects to be appropriately adjusted as the step size is reduced.

The second major change made in the pattern search to improve its efficiency is the elimination of exploratory moves about the end values of an unsuccessful pattern move. In general in this investigation, such exploratory moves did not prove successful. The procedure now is to return to the previous basepoint[2,8,9] and continue the search with exploratory moves at reduced step size. Each time a reduction is made, the step size is reduced by a factor of 2 until the minimum (specified) step size is reached.

The success of the results is demonstrated by comparing Woltosz's results to those obtained with the present program. Woltosz, on a CDC 6400 computer, obtained an optimum design for maximum total impulse/motor weight with 5 variables in somewhat over 1 hour of computer operating time.[9] In the demonstration with the present program which follows, more or less optimum thrust-time traces with 10 variables are obtained on the IBM 3031 in less than 34 minutes of computer operating time.

Program Inputs

The program inputs and outputs are now discussed in conjunction with a demonstration of the program. As a test of the program's capabilities,

an attempt is made to match the thrust versus time trace obtained from the static test of the first Space Shuttle SRM (DM-1) starting with input values of 10 variables, all except two of which are 10% below the values used to represent the DM-1 configuration in the simplified design analysis program. For a reason which will be given later, Al is set to a value which is 10% above and DI is set to a value 1% below the corresponding values for DM-1. The invariant design parameters are set at the values used to represent the as-built configuration.

Starting configuration. Brief definitions of all inputs for the starting configuration are given in the program listing. More detailed discussions of these inputs are given in previous reports[4,10,11] and will not be repeated here. However, certain changes to the original input parameters and special rules that must be observed should be mentioned. These are:

ALPHA and BETA now represent the constant coefficients in the modified flame height burning rate equations, Eqs. III-4 and 5, respectively. When ALPHA is 0, the simpler burning rate law $r=aP^n$ applies.

The input L now represents the estimated total port length of the final configuration. Because a number of the internal program constraints are based on this value and because it is also presently a fixed parameter in the burning rate law, a reasonable estimate should be made. Also, all starting values of the variable design parameter must lie within the limits set by the constraints. Finally, the starting values are now input in NAMELISTS for which the program listing provides the necessary guide.

Program control inputs. Figure IV-2 shows the printout of the program control inputs which are now defined and discussed:

OPTFLG establishes the optimization criterion to be used. OPTFLG =

1 to maximize the ratio of total impulse to motor weight

2 to mimimize the motor weight

3 to match thrust versus time data

KSWTCH indicates which parameters are to be optimized. Set KSWTCH(I) equal to 1 to allow the optimization of parameter I. If KSWTCH(I) = 0, parameter I will remain fixed. The set of parameters available for optimization and their corresponding KSWTCH locations (I) are given in Table IV-1. Thus, for the demonstration program as indicated at the top of Fig. IV-2, the parameters to be varied during the search are DTI,LTAP, ZO, DI, Al, THETAG, LGCI, LGNI, LGSI and TAUS. The parameters which remain constant at their starting values are DE, ALFAN, XT and FILL. The parameters TAUWS and TAUWW are not applicable to this design which uses a truncated tip star grain segment; however, KSWTCH(15) and KSWTCH(16) should be set equal to 0. Also, KSWTCH(17) through (25) must also be set to 0. Storage space is reserved in the program to provide for possible future

```
        PROGRAM CONTROL INPUTS
OPTFLG=   3
KSWTCH(I)=   1   0   0   1   0   1   1   1   1   1   1   1   0   1   0   0
ALFMIN=   10.000                  ALFMAX=   20.000
TPMN=  0.20000                    TPMX=  0.84000
A1MN=0.030000                     A1MX=0.055000
FILLMN=    0.500                  FILLMX=    5.000
FWEBMN=0.200000                   FWEBMX=0.800000
SFWEMN=  5.00000                  SFWEMX=10.00000
DEMX=   150.000
DVREQ=   5800.00

DEL= 1.00000                      DELMIN=0.100000
ITLIM=    14
IPT=   1
IOUT=   2
```

THRUST-VS-TIME POINTS TO BE FIT: (FACTOR=0.1E-07)

TIME	THRUST	WEIGHT FACTOR
1.0000	2679422.0	1.0
10.0000	2872731.0	1.0
20.0000	2929733.0	1.0
25.0000	2798030.0	1.0
32.5000	2514919.0	1.0
40.0000	2298426.0	1.0
57.5000	2073226.0	1.0
67.5000	2193260.0	1.0
77.5000	2271043.0	1.0
82.5000	2196400.0	1.0
90.0000	2028144.0	1.0
100.0000	1927222.0	1.0
105.0000	1814303.0	1.0
110.0000	1653717.0	1.0
113.0000	1481576.0	1.0
115.0000	1329683.0	1.0
116.0000	1136972.0	0.1
123.0000	108225.0	0.1

Fig. IV-2. Program control and desired thrust vs. time inputs for SRMDOP demonstration program.

Table IV-1. Parameters available for optimization and their corresponding KSWTCH locations.

I	Parameter	I	Parameter
1	DTI	9	THETAG
2	DE	10	LGCI
3	ALFAN	11	LGNI
4	LTAP	12	LGSI
5	XT	13	FILL
6	ZO	14	TAUS
7	DI	15	TAUWS
8	A1	16	TAUWW

addition of nine parameters with these latter KSWTCH locations. These last nine KSWTCH(I) values are not presently printed with the other program control inputs.

ALFMIN and ALFMAX are the minimum and maximum allowable limits of the nozzle exit half angle ALFAN in degrees, respectively. Limits of 10° and 20°, respectively, are recommended for a straight conical nozzle. If a bell-shaped nozzle is contemplated, ALFMIN should be somewhat lower.

TPMN and TPMX are the minimum and maximum allowable limits on the throat-to-port area ratio, respectively. These control the range of DTI. The limit TPMN should be selected with a viewpoint toward attaining reasonable volumetric efficiency. Consideration should be given to the erosive burning characteristics of the propellant when specifying TPMX.

A1MN and A1MX are the minimum and maximum allowable burning rate coefficients A1 in $in/sec\text{-}psia^n$, respectively. Corresponding propellant densities, processing characteristics and strengths should be considered in selecting these limits.

FILLMN and FILLMX are the minimum and maximum allowable limits, respectively, on the star grain fillet radius FILL in inches. Stress considerations would ordinarily govern selection of FILLMN while FILLMX should be selected with a view towards obtaining reasonable volumetric loading density.

FWEBMN and FWEBMX are, respectively, the minimum and maximum allowable web fractions (1-DI/DO) for a c.p. grain or grain segment. Since DO is

fixed, the value of web fraction is controlled by the average initial internal grain diameter DI for each configuration. The minimum should be selected with volumetric loading density again in mind while the maximum should be selected in relation to the estimated ultimate value of DTI to avoid excessive erosive burning problems.

SFWEMN and SFWEMX are, respectively, the minimum and maximum allowable star grain web-thicknesses (TAUS, TAUWS or TAUWW) in inches. The lower limit will usually be based upon the desired total burning time with due regard to the value or range of burning rates specified. The user should remember that computer operating time in general can be greatly reduced by specifying reasonable ranges of values, especially when the accuracy of the starting value is in question. SFWEMX might likewise be determined based on desired burning time with some consideration of the general trace shape characteristics obtained with thick-webbed star grains.

DEMX is the maximum allowable nozzle exit diameter DE in inches. The program internally constrains DE $\geq$ 2 (DTI).

DVREQ is the minimum required ideal vehicle velocity in ft/sec. This variable is used only when OPTFLG = 1 or 2.

DEL is the initial step size for the pattern search. A DEL of 1.0 corresponds to a 5% change in the optimization variables for both exploratory and pattern moves.

DELMIN is the minimum allowed DEL. The stepsize is halved whenever a series of moves fails to produce improvement in the objective function. The search is terminated when the stepsize becomes less than DELMIN.

ITLIM is the maximum number of pattern moves allowed before the search is terminated. This provides the user an additional control over the extent of the search.

IPT controls the amount of data on the details of the search that appears in the program printout. IPT =

1 for printout of values of each variable used at each step of the search, the value of objective function obtained with each move, and identification of basepoints and types of moves (exploratory or pattern).

0 for minimum output. Only the values corresponding to basepoints and pattern moves are printed. The final values of the variables are also printed.

-1 for a printout consisting only of the final results; i.e., values of variables and the objective function.

IOUT controls the printout of ballistic data. The printouts when obtained, follow generally the format of the simplified design analysis

program.[10,11] This includes listing of the values of all design parameters, both fixed and variable, and a number of time varying parameters of interest, e.g., thrust, nozzle and stagnation pressure, head end pressure, propellant strain, maximum flow Mach number and burning surface area.
IOUT =

0 for no output configurations.

1 for only the initial configuration.

2 for only the final configuration.

3 for both initial and final configurations.

Values of all of the above program control inputs are furnished to the program by means of a single NAMELIST.

Desired thrust versus time. Data for the thrust versus time trace to be matched is read into the program on data cards in the format indicated by the program listing. This data is, of course, required only for OPTFLG = 3. The parameters for which values must be furnished are now defined and discussed. A printout of the data furnished for the program demonstration is given at the bottom of Fig. IV-2.

NFVST is the number of thrust-time points to be input. As many points should be used as is necessary to give clear definition to the trace characteristics desired. Space is presently reserved in the program for 20 data points.

TP(I) and FVS(I) are, respectively, the time and thrust of data point I.

XI(I) is the weight factor to be assigned in the objective function (Eq. IV-1) to data point (I). This input can be used to assign relative importance to obtaining design goals for various portions of the trace. Also it can be used to prevent the search from being misled because of inaccuracy in the modeling of the ballistics. For example, in the demonstration program relatively low values have been assigned for the last two data points. This is because the program presently does not model nozzle flow separation such as occurs at low pressure under the conditions of the DM-1 static test. This defect can be easily corrected in future work but for the present its impact on the results is minimized by the expedient of assigning low values of XI(I) for the last two points.

FACTOR is used to keep the magnitude of the objective function at a reasonable value. For motors in the three-million-pound class a value of 10^{-8} is recommended which should give final objective functions in the range of 10^{2} to 10^{3}.

Program Outputs

A sample of the data that can be printed out giving the details of the pattern search is given by Fig. IV-3 for the program demonstration example. This output is obtained only when IPT = 1 as previously discussed. Regardless of the value of IPT (or IOUT) specified, the initial and final values of thrust calculated from the internal ballistic portion of the program are printed along with corresponding values of the desired thrust (FVS(I) at the input time data points TP(I)). Percent differences are also tabulated. This is illustrated in Fig. IV-4 for the example problem. Additional calculated internal ballistic data can be obtained by use of the program options IOUT = 1, 2 or 3, as previously discussed.

Results of the Demonstration Example

The results for the example problem are best summarized by a comparison of the final values of the variable design parameters with those of the as-built representation of DM-1 configuration. This is done in Table IV-2 where the starting values and percent difference between final and as-built values are also given. It is seen that the final values are for the most part within a few percent of the as-built values. One exception is Z0 where a substantial difference exists. This discrepancy arises because of the inability of the simplified design analysis to properly model the taper of the two central and identical c.p. grain segments in the DM-1 as discussed in Section III of this report. A similar difficulty arises with THETAG because the actual aft end configuration of the Space Shuttle SRM can only be approximated with this variable. This is the reason reference is made to the as-built representation.

Table IV-2 also gives the objective function (OBJ) for the three configurations evaluated by SRMDOP including the as-built representation. It is seen that the final values obtained from the search yield a slightly lower OBJ than that of the as-built representation. This is to be expected since the final values are obtained as a result of a search wherein the 10 optimization variables are free to adjust their values to attempt to compensate for differences between desired and calculated thrust that result from deficiencies in the modeling. Nevertheless, the modeling is good enough and the objective functions are low enough in both cases to provide assurance that, if two SRM's were built to the two different sets of specifications, the performance of each would be very close to that desired.

An additional summary of the program results is a plot of head end chamber pressure versus time for the initial and final configurations of the SRMDOP demonstration superimposed on a plot of DM-1 static test data points (Fig. IV-5). No plotting routine is provided by SRMDOP so the plot was obtained using the simplified design analysis program modified for grain deformation effects[3] and further modified to accommodate the new burning rate model discussed in this and the previous Section of this report. Figure IV-5 shows that the actual chamber pressure as well as the thrust of the DM-1 are matched well by the final design furnished by SRMDOP.

```
  , OBJ:     4.823109E+03   TR.
                                        1.106718E+03  5.094000E+0.  .....173E+02  7.920000E+00
 210 OBJ:    4.842395E+03   TRIAL:      5.339536E+01  2.225677E+02  2.900000E+00  5.557173E+01  4.212181E-02  1.413717E-01
                                        1.106718E+03  5.094000E+01  1.719173E+02  7.821000E+00
 210 OBJ:    4.804184E+03   TRIAL:      5.339536E+01  2.225677E+02  2.900000E+00  5.557173E+01  4.212181E-02  1.413717E-01
                                        1.106718E+03  5.094000E+01  1.719173E+02  8.019000E+00
****      5
****      3
     OBJ:    4.823109E+03   DEL:2.500E-01
                                 ..............................................................................................
                                           DTI           LIAP           ZO            OI             AL           THFLAG
                                           LGCI          LGNI           LGSI          TAUS
B A S E   P O I N T : ----->            5.339536E+01  2.225677E+02  2.900000E+00  5.557173E+01  4.212181E-02  1.413717E-01
                                        1.106718E+03  5.094000E+01  1.719173E+02  7.920000E+00
P A T T E R N   --------------->        5.473665E+01  2.253704E+02  2.900000E+00  5.553923E+01  4.157795E-02  1.413717E-01
                                        1.147975E+03  5.094000E+01  1.762515E+02  7.920000E+00
     OBJ:    7.028555E+03   DEL:2.500E-01
 2 1 OBJ:    7.108117E+03   TRIAL:      5.542085E+01  2.253704E+02  2.900000E+00  5.553923E+01  4.157795E-02  1.413717E-01
                                        1.147975E+03  5.094000E+01  1.762515E+02  7.920000E+00
 2 1 OBJ:    4.266398E+03   TRIAL:      5.405243E+01  2.253704E+02  2.900000E+00  5.553923E+01  4.157795E-02  1.413717E-01
                                        1.147975E+03  5.094000E+01  1.762515E+02  7.920000E+00
 2 2 OBJ:    4.161117E+03   TRIAL:      5.405243E+01  2.281876E+02  2.900000E+00  5.553923E+01  4.157795E-02  1.413717E-01
                                        1.147975E+03  5.094000E+01  1.762515E+02  7.920000E+00
 2 3 OBJ:    4.083274E+03   TRIAL:      5.405243E+01  2.281876E+02  2.936249E+00  5.553923E+01  4.157795E-02  1.413717E-01
                                        1.147975E+03  5.094000E+01  1.762515E+02  7.920000E+00
 2 4 OBJ:    4.015494E+03   TRIAL:      5.405243E+01  2.281876E+02  2.936249E+00  5.623346E+01  4.157795E-02  1.413717E-01
                                        1.147975E+03  5.094000E+01  1.762515E+02  7.920000E+00
 2 5 OBJ:    3.219135E+03   TRIAL:      5.405243E+01  2.281876E+02  2.936249E+00  5.623346E+01  4.105823E-02  1.413717E-01
                                        1.147975E+03  5.094000E+01  1.762515E+02  7.920000E+00
 2 6 OBJ:    3.217513E+03   TRIAL:      5.405243E+01  2.281876E+02  2.936249E+00  5.623346E+01  4.105823E-02  1.431388E-01
                                        1.147975E+03  5.094000E+01  1.762515E+02  7.920000E+00
 2 6 OBJ:    3.220956E+03   TRIAL:      5.405243E+01  2.281876E+02  2.936249E+00  5.623346E+01  4.105823E-02  1.396045E-01
                                        1.147975E+03  5.094000E+01  1.762515E+02  7.920000E+00
 2 7 OBJ:    3.621739E+03   TRIAL:      5.405243E+01  2.281876E+02  2.936249E+00  5.623346E+01  4.105823E-02  1.413717E-01
                                        1.162324E+03  5.094000E+01  1.762515E+02  7.920000E+00
 2 7 OBJ:    6.469285E+03   TRIAL:      5.405243E+01  2.281876E+02  2.936249E+00  5.623346E+01  4.105823E-02  1.413717E-01
                                        1.133625E+03  5.094000E+01  1.762515E+02  7.920000E+00
 2 8 OBJ:    3.188097E+03   TRIAL:      5.405243E+01  2.281876E+02  2.936249E+00  5.623346E+01  4.105823E-02  1.413717E-01
                                        1.147975E+03  5.157675E+01  1.762515E+02  7.920000E+00
 2 9 OBJ:    3.082870E+03   TRIAL:      5.405243E+01  2.281876E+02  2.936249E+00  5.623346E+01  4.105823E-02  1.413717E-01
                                        1.147975E+03  5.157675E+01  1.784546E+02  7.920000E+00
 210 OBJ:    3.066769E+03   TRIAL:      5.405243E+01  2.281876E+02  2.936249E+00  5.623346E+01  4.105823E-02  1.413717E-01
                                        1.147975E+03  5.157675E+01  1.784546E+02  8.019000E+00
 210 OBJ:    3.098539E+03   TRIAL:      5.405243E+01  2.281876E+02  2.936249E+00  5.623346E+01  4.105823E-02  1.413717E-01
                                        1.147975E+03  5.157675E+01  1.784546E+02  7.821000E+00
****      6
****      4
     OBJ:    3.082870E+03   DEL:2.500E-01
                                 ..............................................................................................
                                           DTI           LIAP           ZO            OI             AI           THFLAG
                                           LGCI          LGNI           LGSI          TAUS
B A S E   P O I N T : ----->            5.405243E+01  2.281876E+02  2.936249E+00  5.623346E+01  4.105823E-02  1.413717E-01
                                        1.147975E+03  5.157675E+01  1.784546E+02  7.920000E+00
P A T T E R N   --------------->        5.472264E+01  2.339198E+02  2.973223E+00  5.690842E+01  3.997337E-02  1.413717E-01
                                        1.190057E+03  5.222623E+01  1.851227E+02  7.920000E+00
     OBJ:    6.732965E+03   DEL:2.500E-01
     OBJ:    3.405114E+03                  ...01  2.339198E+..                ...90842E+01  3.9...
```

Fig. IV-3. Sample of pattern search data from SRMDOP (IPT=1).

INITIAL DESIGN

TIME	DESIRED F	PREDICTED F	PERCENT ERROR
1.0000	2679422.00	3124709.00	16.6188
10.0000	2872731.00	3382724.00	17.7529
20.0000	2929733.00	3144837.00	7.3421
25.0000	2798030.00	2883218.00	3.0446
32.5000	2514919.00	2559755.00	1.7828
40.0000	2298426.00	2308600.00	0.4427
57.5000	2073226.00	2452510.00	18.2944
67.5000	2193260.00	2304714.00	5.0817
77.5000	2271043.00	2139497.00	-5.7923
82.5000	2196400.00	2006638.00	-8.6397
90.0000	2028144.00	1783062.00	-12.0840
100.0000	1927222.00	372776.312	-80.6573
105.0000	1814303.00	0.0	-100.0000
110.0000	1653717.00	0.0	-100.0000
113.0000	1481576.00	0.0	-100.0000
115.0000	1329683.00		
116.0000	1136972.00		
123.0000	108225.000		

FINAL DESIGN

TIME	DESIRED F	PREDICTED F	PERCENT ERROR
1.0000	2679422.00	2659088.00	-0.7589
10.0000	2872731.00	2841810.00	-1.0764
20.0000	2929733.00	2935675.00	0.2028
25.0000	2798030.00	2777144.00	-0.7465
32.5000	2514919.00	2475938.00	-1.5500
40.0000	2298426.00	2250952.00	-2.0655
57.5000	2073226.00	2043279.00	-1.4445
67.5000	2193260.00	2178288.00	-0.6826
77.5000	2271043.00	2190785.00	-3.5340
82.5000	2196400.00	2143954.00	-2.3878
90.0000	2028144.00	2061195.00	1.6296
100.0000	1927222.00	1865245.00	-3.2159
105.0000	1814303.00	1752942.00	-3.3821
110.0000	1653717.00	1625570.00	-1.7020
113.0000	1481576.00	1575547.00	6.3426
115.0000	1329683.00	1284086.00	-3.3690
116.0000	1136972.00	1069605.00	-5.9251
123.0000	108225.000	0.0	-100.0000

Fig. IV-4. Initial and final thrusts vs. time for SRMDOP demonstration program.

Table IV-2. Comparison of starting and final values with the values representing the as-built configuration of the DM-1 for the demonstration program.

(1) Variable (See Fig. IV-1)	(2) Starting Value	(3) Final Value	(4) As-Built Representation	% Difference (3) vs. (4)	% Difference Alternative Design† vs. (4)
DTI, in.	48.988	54.052	54.420	-0.7	-.144
LTAP, in.	219.82	258.28	244.25	+5.7	+12.3
ZO, in.	2.90	2.41	3.27	+26.3	+8.5
DI, in.	59.27	60.57	59.87	+1.2	+3.9
Al, in/sec-psia^n	0.0449	0.0411	0.0409	+0.5	-10.0
THETAG, °	8.10	8.10	9.00	+10.0	+10.0
LGCI, in.	1027.17	1130.94	1141.13	-0.8	-0.8
LGNI, in.	50.94	55.62	56.60	-1.7	-9.0
LGSI, in.	159.55	171.39	177.28	-3.3	-9.1
TAUS, in.	7.92	9.03	8.80	+2.5	-0.6
OBJx10^{-3}	133.19	.389	0.710	-45.2	-73.1
Mtr. Wgt.x10^{-6}, lbm.	0.998	1.087	1.106	-1.7	‡
PMAX, psia	1154.	844.	835.	+1.1	‡
Comp. Time, min.	____	33.15	____	____	____

†Starting values for the alternative design are the same as (2) except Al=0.03678.

‡Final ballistic and motor weight data were not printed for the alternative design (IOUT=0).

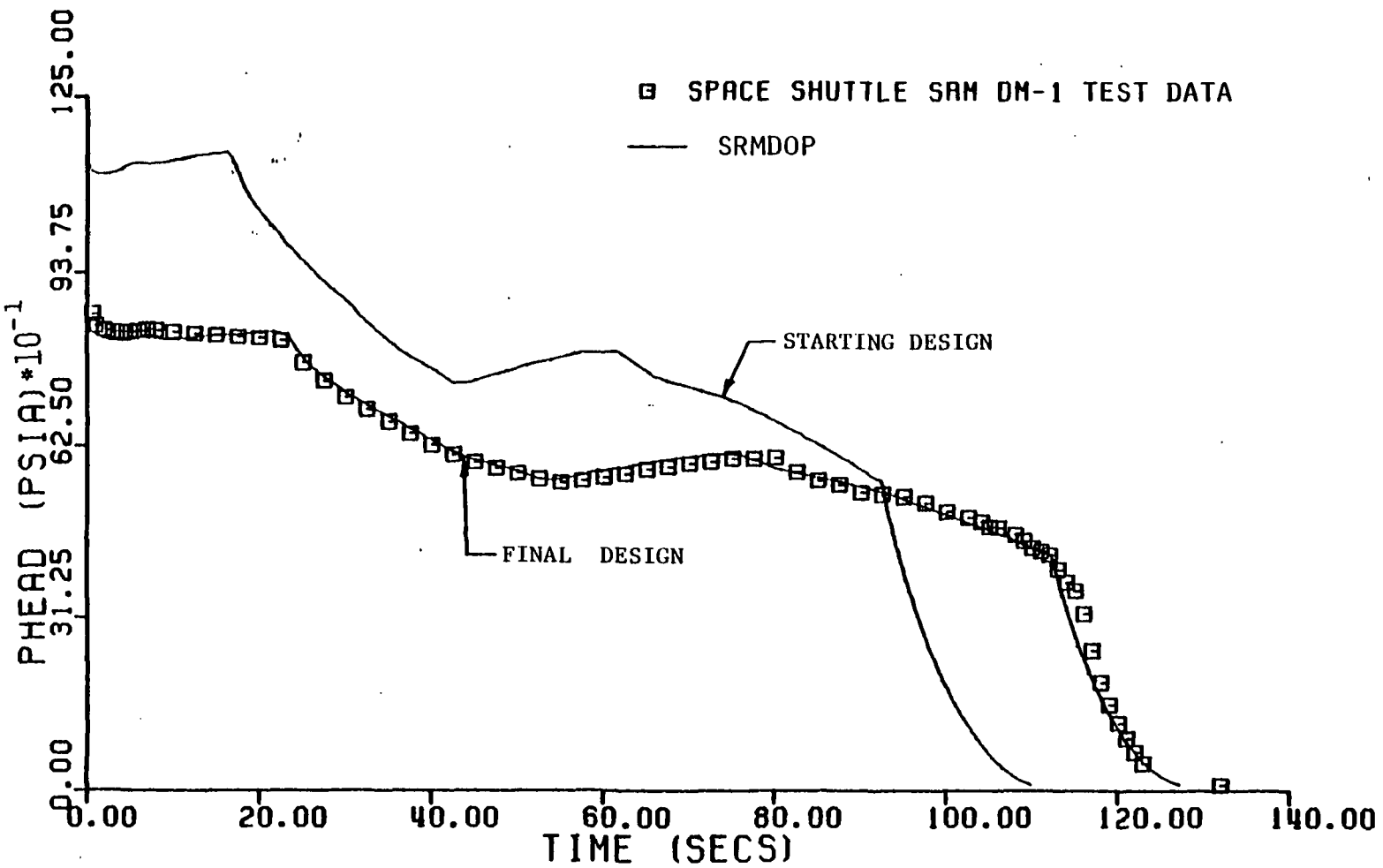

Fig. IV-5. Head end chamber pressure versus time from DM-1 static test data and from SRMDOP.

Discussion

The results of the demonstration show SRMDOP offers an approach to preliminary design of SRM's that has great potential for simplifying and shortening the design process. However, the designer must first develop an understanding of the program and how it responds. Rules to be observed to avoid certain pitfalls have been pointed out, but it is to be expected that some experience with the program will be required before the user can achieve desired results. For example, when tabular values are required to specify portions of the burning surface, special consideration needs to be given to dividing the burning surface properly into those sections to be represented by equations and those that are represented by tabular values.

One difficulty occurs in the first attempt to conduct this demonstration that indicates at first a weakness but later a strength of the program. This difficulty is encountered when the value of all 10 variable design parameters are input 10% below the as-built values. The low burning rate combines with the low value of throat area DTI in such a way that after a few moves in the search, a rather low value of the objective function is obtained with a low burning rate compensating for a low DTI. The program then proceeds to optimize the other variables around these values of DTI and Al with a final OBJ value of 465. This is evidence of a tendency of the program to seek out local minima rather than the true or global minimum. The particular minima towards which the program converges depends on the starting values of the variable design parameters. For the demonstration, it is necessary to show that the program can converge toward the as-built configuration from off-design values. Good results are obtained by starting with an Al that was 10% higher rather than 10% lower and DI that was only 1% lower than the as-built values. This, as previously shown, gives an OBJ of 389 which is lower than that for the as-built representation. It is also lower than that which results from starting values that are all 10% lower than the as-built design.

A lower OBJ does not necessarily indicate better convergence towards the as-built design. Indeed, when the program is started with all values 10% below the as-built values except for DI which is started at 1% less than its as-built value, an OBJ of 191 is obtained. The corresponding percentage deviations of the final values of the design parameters from the as-built values are given in the last column of Table IV-2 under the heading of "alternative design." It is seen that the deviations are substantial although the lower value of the objective function shows a superior trace match is obtained.

The strength of SRMDOP that the difficulty encountered in the demonstration brings out is this: By using a number of sets of starting variables, a number of designs can be found that will satisfy to varying degrees the performance requirements specified within the limits imposed by the goodness of the mathematical model of the internal ballistics. The designer is then free to make a final selection based upon consideration of other characteristics as well as the objective function. For example,

he might decide that the smaller throat of the "alternative design" might be desirable and the lower OBJ of this design would provide some assurance that a better trace shape would be obtained than with the final design parameters of the primary demonstration.

Once the designer has gained experience with the program, there are a variety of other uses to which it may be put. For example, simple single or double variable optimizations can be conducted for the purpose of determining how to alter an existing design to achieve more desirable thrust-time trace characteristics. Also, the program might be used to deduce from test data the apparent burning rate coefficient Al based on either $r=aP^n$ with ALPHA=0 or the new modified flame height burning rate model. Alternative burning rate laws could also be used by program modification of the burning rate equation.

Of course, improvements of the program are possible. An obvious one that has been discussed earlier is to incorporate in SRMDOP a simple model of flow separation during tailoff as was previously done for ignition calculations in the simplified design analysis program.[2] Another improvement which would add to the flexibility of the program would be to include the outside diameter of the propellant (DO for c.p. grains) as a design variable. The changes necessary would be somewhat involved, especially for configurations that involve both c.p. and star segments, but there is no reason this could not be done. Presently, the designer can, of course, investigate the potential of various grain diameters through several runs with various fixed DO and corresponding diameters for star grain segments.

V. CONVECTIVE HEATING OF PROPELLANT DURING IGNITION

SRM ignition transient analyses have been conducted with various degrees of complexity ranging, for example, from simplified lumped-parameter analyses[11,15] to much more complex spatial analyses.[12,16] The simplified analyses treat the propellant ignition and flame spreading as phenomenological events and, therefore, these parameters must be completely specified prior to the ignition transient analysis. The more complex analyses[12,16] incorporate the computations of these parameters by means of appropriate heat transfer, thermodynamic and fluid flow relations. Generally, the more complex analyses result in greater accuracy of prediction. However, some relatively unknown or uncertain processes may be inappropriately or inaccurately modeled.

The analytical prediction of convective heating of the propellant surface to produce ignition may be one of the more uncertain processes of Refs. 12 and 16, as is the convective heating prediction of any surface, especially one with complex geometry. A semi-empirical relationship, employing a few relatively uncertain physical and geometrical correction factors, is used to determine the convective heat transfer coefficient between the hot combustion gases and the unignited propellant surface. A more thorough analysis, both theoretical and empirical, of the convective coefficient might provide a better understanding of the heat transfer process created by the hot gas during ignition and would thus aid future investigations of ignition transients and possibly other similar phenomena. It is the purpose of the present analysis to semi-empirically investigate the convection process in order to better predict the actual ignition transient. This will be accomplished by using a pattern search technique to determine the convective coefficients needed to match a test data ignition transient.

The semi-empirical convective relationship used in Refs. 12 and 16 is deduced from the conventional Dittus-Boelter correlation for fully developed turbulent flow in smooth pipes. Corrections for entrance effects and variations of the physical properties of the combustion gases across the boundary layer yields:[17]

$$h = c\, P_r^{-0.6}\, c_p\, \left(\frac{Pu}{R}\right)^{0.8} W^{0.1}\, T_{af}^{-0.67}\, (x_{seg}\, d_h)^{0.1} \qquad \text{(V-1)}$$

where c has the value 0.0346, P_r is Prandtl number, c_p is specific heat at constant pressure, P is pressure, u is gas velocity, R is the specific gas constant of the combustion gases, W is the molecular weight of the combustion gases, T_{af} is the average film temperature, x_{seg} is the effective distance from the leading edge of the segment being considered and d_h is the hydraulic diameter of the port.

This relationship appears to be appropriate since the surface of the solid propellant resembles a smooth surface, and is non-ablative before

the surface is ignited. Therefore, the thermodynamic and hydrodynamic boundary layers should closely resemble those of a smooth pipe and, presumably, adjustments are implicit in the relationship for the most important thermodynamic, fluid flow and geometry changes along the length of the motor and between different motors.[17] However, the accuracy of these adjustments for even a given motor is questionable, and the overall result may be a convective coefficient that is inadequate in establishing true heat transfer rates. Additionally, radiation from the igniter and main motor combustion gases contributes to the total heat transfer to the surface, but is not included in the analyses of Refs. 12 and 16. As a first approach, it is assumed that the radiation-to-convection ratio remains relatively constant between motors. Then the total of the inaccuracies of the convective relationship and the effect of radiation can be included in the constant coefficient of the relationship (Eq. V-1).

In order to determine the set of constant coefficients applicable, a procedure similar to that which is described in Section IV, by which a set of main SRM design parameters are fixed, is developed. That is, by determining the "best" constant coefficients, the difference between the predicted and actual ignition transients can be minimized. Assuming that the remainder of the model used in Refs. 12 and 16 is phenomenologically accurate, this amounts to minimizing the difference between the predicted and actual heat transfer rates.

The computer analyses of Refs. 12 and 16 subdivide the motor into a number of segments down the length of the motor and compute the convective heating, flame spreading and contributions to the total ignition transient for each segment individually. Coupling a pattern search technique[8] to this analysis, and minimizing the difference between the predicted ignition transient and actual test data, now enables the individual adjustment of the constants in the convective coefficient relationships for each segment. This results in the determination of a set of "best" values of the constants for all the motor segments. However, the computational time requirements for this procedure with a large number of segments are prohibitive since the ignition transient prediction analyses of Refs. 12 and 16 must be executed a large number of times, and a single 320-msec. transient prediction requires approximately three minutes of execution time on an IBM 370. This time requirement is primarily a result of the small time steps required (from stability considerations) to solve the governing partial differential equations using an implicit central difference scheme. The only feasible solution is to reduce the number of optimization variables (the constants in the convective coefficient relationship(s))to a reasonable number. This is accomplished by systematically grouping the motor segments and using a common constant for each group.

Figure V-1 shows schematically how the Space Shuttle SRM is divided by the analysis into 24 equal-length segments.[12,16] These segments are now combined into 4 groups having common convective coefficient constants (c_1, c_2, c_3, c_4). More attention is given to the head end of the motor since the igniter plume impinges on the first segment and since the head-end and immediately adjacent segments are more critical to the overall

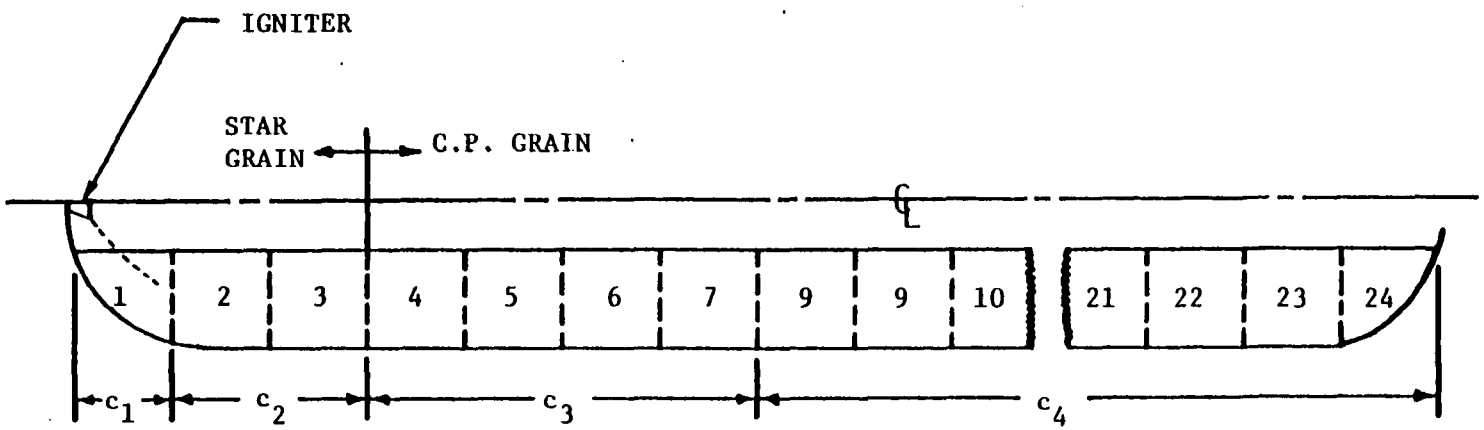

Fig. V-1. Schematic of Space Shuttle SRM divided into 24 equal-length segments with 4 convective coefficient groups (c_1-c_4).

ignition transient. As shown on Fig. V-1, the head-end star grain of the Space Shuttle SRM is contained in the first three motor segments and two of the four convective coefficient constants are assigned to this star grain while the other two constants are assigned to the rest (21 segments) of the motor.

Test data from the Space Shuttle DM-2 is plotted in Fig. V-2 along with a typical prediction using the analyses of Refs. 12 and 16 with convective coefficient constants as follows:

SEGMENT(S)	COEFFICIENT (c)
1	1.4 (0.0346) = 0.0484
2	1.3 (0.0346) = 0.0450
3	1.2 (0.0346) = 0.0415
4	1.1 (0.0346) = 0.0318
5-24	1.0 (0.0346) = 0.0346

The objective function, which is the sum of squares of the difference between each test data pressure value and the predicted pressure at the same time point, for this prediction is 509.7×10^3. Using the pattern search technique to minimize the objective function, a new set of convective coefficient constants is found which generates the "best" (optimum) prediction in Fig. V-2 with an objective function of 59.16×10^3. The optimum constants are:

SEGMENT(S)	COEFFICIENT
1	$c_1 = 0.0401$
2-3	$c_2 = 0.0307$
4-7	$c_3 = 0.0116$
8-24	$c_4 = 0.0512$

Note that the constants are reduced (from the previous analysis) over the head-end portion of the transient, which allows a longer time delay before ignition, and thus a better fit of the initial portion of the transient. But also note that the constant for segment one is larger than the next two constants, probably because the igniter plume impingement occurs on the first segment. The aft end of the motor now exhibits a very high constant (and consequently a very high convective heat transfer coefficient), but it will be shown that this portion of the motor has a relatively insignificant effect on the overall transient. Thus, the convective coefficient constant over the aft portion of the motor may be artificially inflated and should probably be forced to a more reasonable (lower) value.

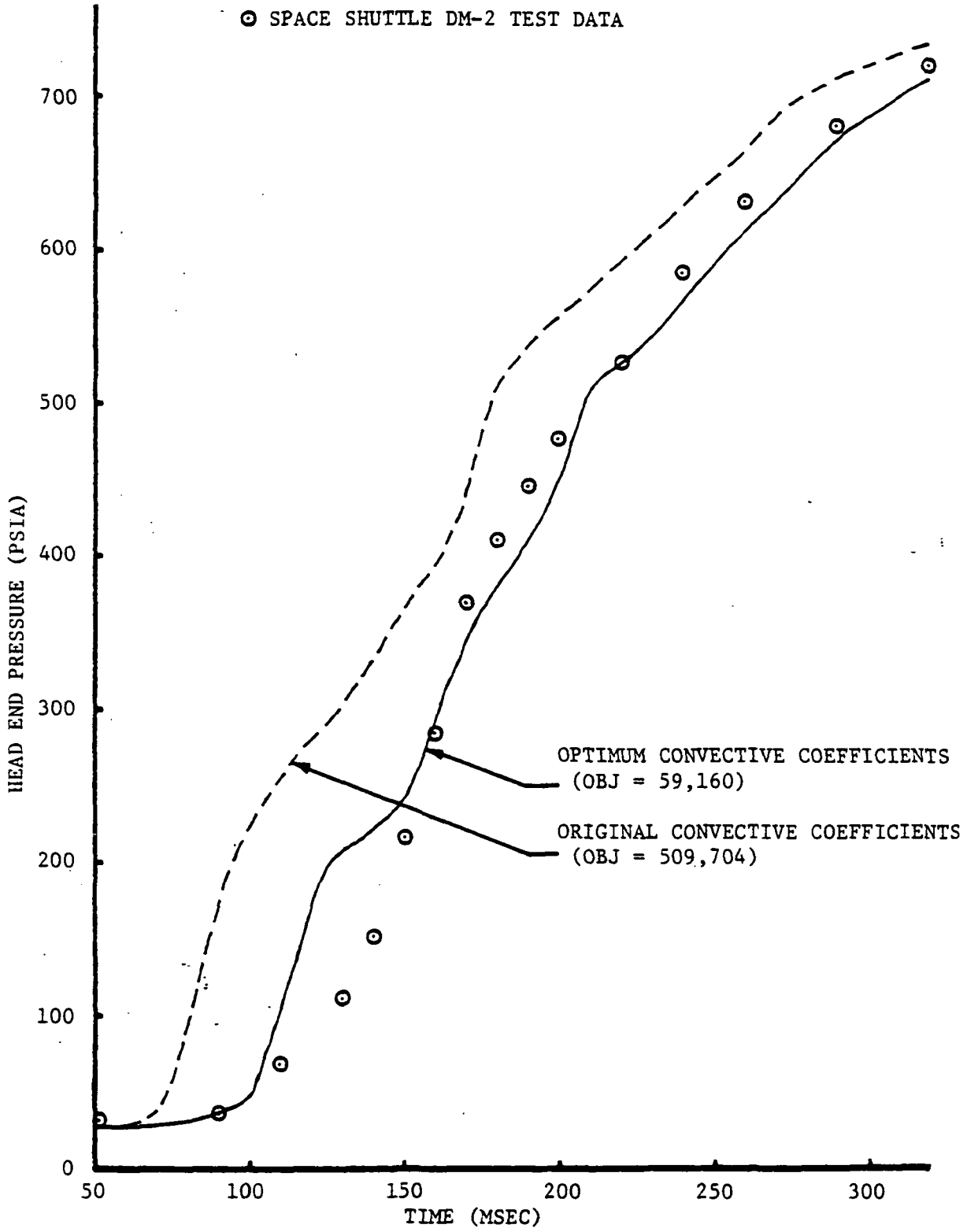

Fig. V-2. Ignition transient predictions for the Space Shuttle DM-2.

To demonstrate the relative sensitivity of the analysis to changes in the convective coefficient constants, each of the four constants are increased individually by 30 percent of their optimum values. DM-2 test data, the optimum prediction, and each of the four perturbated predictions are collectively plotted on Fig. V-3. It is now obvious from visual inspection of the curves and from the numerical values of the objective function that increasing the head-end heat transfer (increasing c_1 and c_2) has the most significant effect on the overall transient by effectively reducing the ignition delay period. Increasing c_3 and c_4 have essentially no effect on ignition delay and also have relatively little effect on the overall transient. This suggests that another set of optimization variables, concentrating even more on the head-end segments, might more accurately describe the convective process.

The optimum ignition transient prediction fits the DM-2 test data fairly well overall, but it should be noted that it does not fit the test data as well as desired over the initial 150 msec and this is the time period over which the convective heating occurs, prior to complete ignition of the motor. However, if the optimization of the coefficients were based on only the initial portion of the transient (up to complete surface ignition) the coefficients would be inappropriately biased and the corresponding optimum prediction would, in general, inadequately represent the remaining portion of the actual ignition transient. The initial departure of the optimum prediction from the actual transient may be due to an inadequacy of the ignition analyses[12,16] or of the convective coefficient groupings used in the optimization process. In any case, the optimization should continue to be performed over a significant portion of the transient, such as the 320 msec used in the present analysis.

Also, it should be noted in Fig. V-3 that the ignition of segments 8-24 is completed before segments 4-7. This situation is created by the presumably fictitiously large heat transfer rates over segments 8-24, as determined by the optimization procedure. Thus flame spreading occurs in more than one direction; but this phenomenon does not occur when the convective coefficients of Refs. 12 and 16 are used. Such anomalous behavior could be produced in an actual motor, but is not likely in the Space Shuttle SRM because of the large port area and the divergently tapered c.p. grain.

It appears, in view of the above considerations, that consideration should be given in future analyses to not only the (two) convective coefficient constants in the head-end star grain, but also to the two variables which control the rate of flame spread over the star point surfaces. The analysis of Ref. 16 includes a method for controlling the time of first ignition and the rate of flame spread within each individual segment (24 segments in the present analysis). This is accomplished by allowing a predetermined percentage of each segment to initially ignite (after being heated to ignition temperature) and then specifying a time period for the flame front to propagate over the remaining exposed surface of the segment. This is justified since the igniter plume generally impinges more directly on the tips of the star points, thus igniting the tips in advance of the

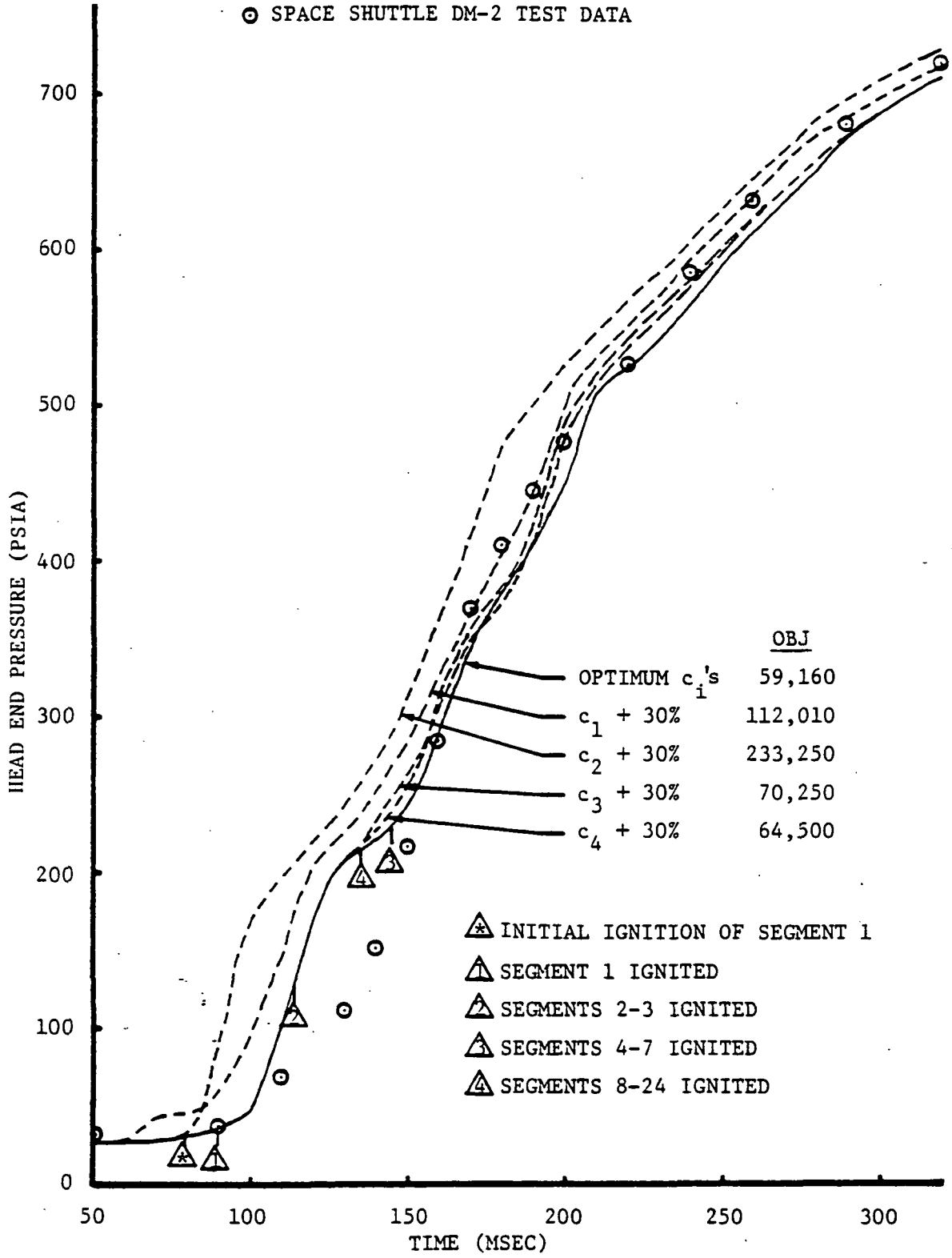

Fig. V-3. Sensitivity of the ignition transient predictions for the Space Shuttle DM-2 to changes in convective coefficients.

star point walls and web. In the present analysis the rate of flame spread (after initial ignition of 10 percent of the star grain surface) has been held constant for all analyses.

The majority of the effort associated with this analysis was involved in coupling the ignition transient analysis of Refs. 12 and 16 with the pattern search routine discussed in Section IV. After debugging the programs, several consecutive, lengthy (one-hour) computer runs were necessary to search out the optimum convective values, since a single transient prediction to 320 msec using the computer program of Refs. 12 and 16 requires approximately three minutes as previously mentioned, and must be executed repeatedly.

Additionally, the present effort includes a literature search in the areas of SRM convective heating and ignition which should prove useful in planned future efforts involving more detailed analysis of the convective heating process. Motors of dramatically different dimensions and propellant grain geometries are to be considered with the hope of establishing some type of semi-empirical relationship between the motors such that possibly a single convective heat transfer relationship will reasonably apply to any size motor using similar ignition techniques. These latter efforts will be those of a graduate student performing research for his Ph.D. in this area.

VI. COMPUTER PROGRAM FOR VISUAL DISPLAY OF TEST DATA

A special task performed under the Cooperative Agreement involves the improvement and extension of a plotting program used at MSFC. The program permits fast, trouble-free plotting of SRM test data on the Tektronix graphics terminals which are tied to the UNIVAC 1108 computer at MSFC. The program is able to read in test data stored on the 1108 and plot it in a regular x vs. y plot, log-log, semi-log, or multiple axis plots (up to 3 ordinate axes, only 1 abscissa). It can read in up to 6 data curves at one time (each containing up to 600 points) and plot them together or separately. A data manipulation routine is available to the user and with it he can add, subtract, multiply, or divide two or more curves together, and calculate thrust rise rate, running average, and obtain a short statistical pointout of data. A variety of other options are available to aid the user in obtaining many forms of calculations or type and style of plot. This program was written to be interactive with the user and written in such a way as to keep the various options available to the user out of the way until he needs them.

The plotting program described was developed by James L. Berry while employed by MSFC as a member of the Cooperative Education Program. Berry, as a laboratory assistant at Auburn University, making use of the MSFC UNIVAC 1108 computer via telephone link, has now completed the following additions or changes to the plotting program:

1. Adding polar plotting capability to the program.

2. Eliminating a minor problem with the subroutine that calculates running averages.

3. Correcting a subroutine that switches data sets from one location to another.

4. Correcting a subroutine used to switch the abscissa values with the ordinate values of a data set.

The capability of the revised program to provide polar plots is illustrated by Fig. VI-1.

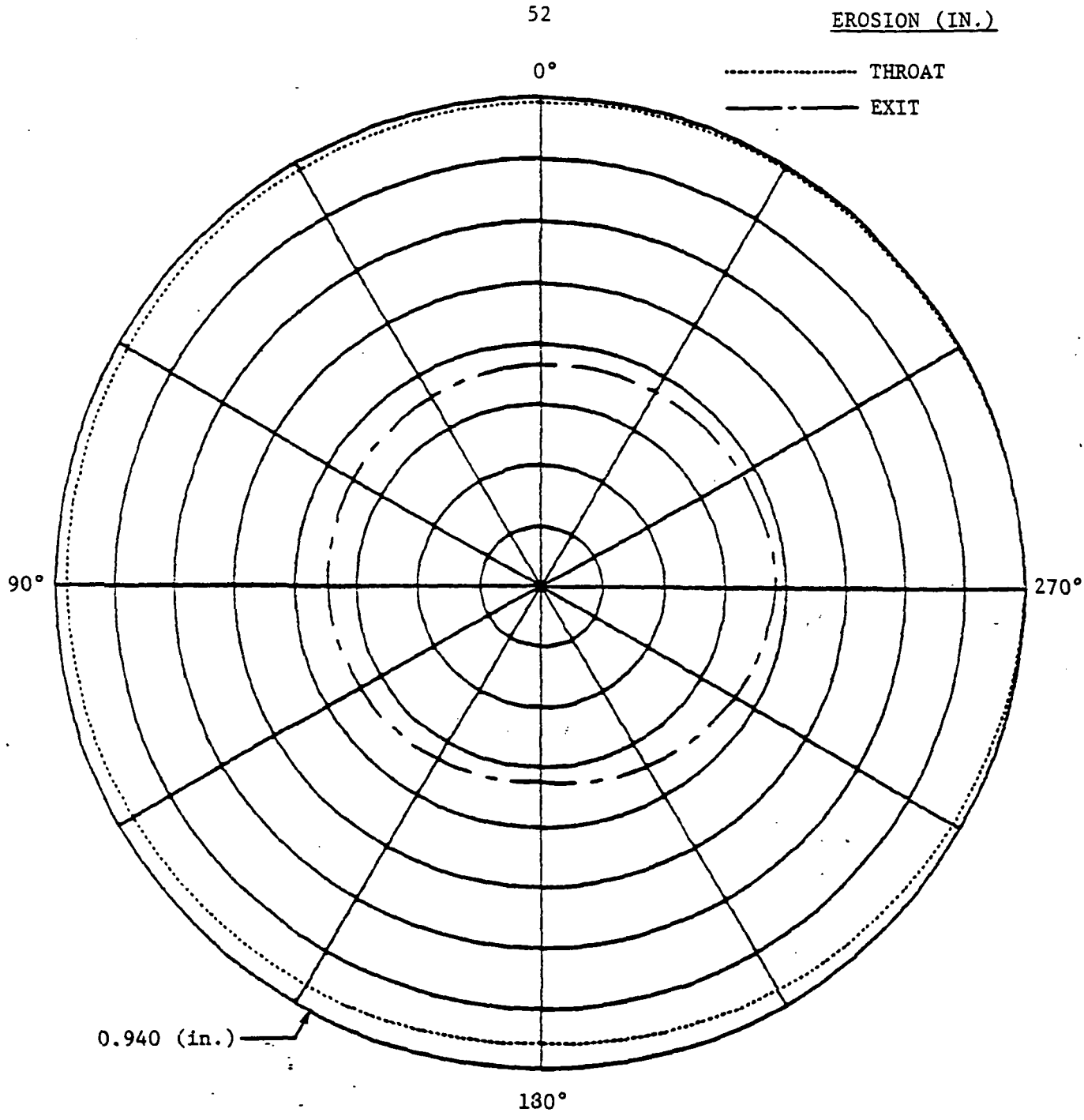

Fig. VI-1. Polar plot of nozzle erosion for Space Shuttle SRM (QM-2).

VII. CONCLUDING REMARKS

The continued research in internal ballistic performance variation has added confidence in previous theoretical analyses of thrust imbalance characteristics between SRM's of a pair. In particular, results of the analyses of the imbalance potential of the Space Shuttle SRM's DM-3 and 4 and QM-1 and 2 are generally within the limits predicted by previous Monte Carlo evaluations.

A general erosive burning relationship has now been established for the simplified design analysis program which should greatly improve the accuracy of predictions at least for SRM's employing PBAN type of propellant. The additional comparisons of predictions with experimental data also tend to confirm both the validity of the hypothesis that grain deformation influences internal ballistic performance and the method by which the effects are taken into account in the revised design analysis program.

The Solid Rocket Motor Design and Optimization Program described should provide the designer with a powerful approach to preliminary design of SRM's that can greatly simplify and shorten the design process.

The investigation of the convective heating of propellant during ignition establishes an approach that has much potential for improving the predictability of ignition transients.

REFERENCES

1. Sforzini, R. H., and Foster, W. A., Jr., "Monte Carlo Investigation of Thrust Imbalance of Solid Rocket Motor Pairs," Journal of Spacecraft and Rockets, Vol. 13, No. 14, April 1976, pp. 198-202.

2. Sforzini, R. H., Foster, W. A., Jr., and Murph, J. E., "Solid Propellant Rocket Motor Internal Ballistics Performance Variation Analysis (Phase Four)," Final Report prepared for NASA, Auburn University, January 1979.

3. Sforzini, R. H., Foster, W. A., Jr., Murph, J. E., and Adams, G. W., Jr., "Solid-Propellant Rocket Motor Internal Ballistics Performance Variation Analysis (Phase Three)," Final Report, NASA Contractor Report CR-150577, Auburn University, November 1977.

4. Sforzini, R. H., and Foster, W. A., Jr., "Solid-Propellant Rocket Motor Internal Ballistic Performance Variation Analysis (Phase Two)," Final Report, NASA Contractor Report CR-150324, Auburn University, September 1976.

5. Sforzini, R. H., and Foster, W. A., Jr., "Solid-Propellant Rocket Motor Ballistic Performance Variation Analyses," Final Report, NASA Contractor Report CR-144264, Auburn University, October 1975.

6. Sforzini, R. H., Foster, W. A., Jr., and Johnson, F. S., Jr., "A Monte Carlo Investigation of Thrust Imbalance of Solid Rocket Motor Pairs," Final Report, NASA Contractor Report CR-210700, Auburn University, November 1974.

7. Foster, W. A., Jr., and Sforzini, R. H., "Optimization of Solid Rocket Motor Igniter Performance Requirements," Paper No. 78-1016, 14th AIAA/SAE Joint Propulsion Conference, Las Vegas, Nevada, July 1978.

8. Hooke, R., and Jeeves, T. A., "Direct Search Solution of Numerical and Statistical Problems," Journal of the Association of Computing Machinery, Vol. 8, No. 2, pp. 212-229.

9. Woltosz, W. S., "The Application of Numerical Optimization Techniques to Solid-Propellant Rocket Motor Design," M.S. Thesis, Auburn University, Auburn, Alabama, March 1977.

10. Sforzini, R. H., "Design and Performance Analysis of Solid-Propellant Rocket Motors Using a Simplified Computer Program," Final Report, NASA Contractor Report CR-129025, Auburn University, October 1972.

11. Sforzini, R. H., "Extension of a Simplified Computer Program for Analysis of Solid-Propellant Rocket Motors," Final Report, NASA Contractor Report No. CR-129024, Auburn University, April 1973.

12. Caveny, L. H., and Kuo, K. K., "Ignition Transients of Large Segmented Solid Rocket Boosters," Final Report, NASA Contractor Report No. CR-150162, Princeton University, April 1976.

13. Sforzini, R. H., Foster, W. A., Jr., and Shackelford, B. W., Jr., "Effects of Propellant Temperature Gradients on the Thrust Imbalance of the Space Shuttle," Journal of Spacecraft and Rockets, Vol. 16, No. 3, May-June 1979, pp. 135-139.

14. Williams, F. A., Barrère, M., and Huang, N. C., Fundamental Aspects of Solid Propellant Rockets, Technivision Services, Slough, England, 1969, pp. 419-434.

15. Sforzini, R. H., and Fellows, H. L., Jr., "Prediction of Ignition Transients in Solid-Propellant Rocket Motors," Journal of Spacecraft and Rockets, Vol. 7, No. 5, May 1970, pp. 636-638.

16. Caveny, L. H., "Extension to Analysis of Ignition Transients of Segmented Rocket Motors," Final Report, NASA Contractor Report No. CR-150632, Princeton University, January 1978.

17. Peretz, A., Caveny, L. H., Kuo, K. K., and Summerfield, M., "The Starting Transient of Solid-Propellant Rocket Motors with High Internal Gas Velocities," Aerospace and Mechanical Sciences Report No. 1100, Princeton University, April 1973.